

EFFECTS OF GRAVITY ON EQUILIBRIUM CRYSTAL SHAPES

by

Apostolos Georgios Gittis

Dissertation submitted to the Faculty of the  
Virginia Polytechnic Institute and State University  
in partial fulfillment of the requirements for the degree of

DOCTOR OF PHILOSOPHY

in

Physics

APPROVED:

---

R. K. P. Zia, Chairman

---

L. N. Chang

---

G. Hagedorn

---

T. K. Lee

---

A. L. Ritter

October, 1988

Blacksburg, Virginia

# EFFECTS OF GRAVITY ON EQUILIBRIUM CRYSTAL SHAPES

by

Apostolos Georgios Gittis

Committee Chairman: R. K. P. Zia  
Physics

(ABSTRACT)

The effects of gravity on the two-dimensional equilibrium shapes (ES) of crystals and menisci are investigated for different geometries (positions) of the substrate.

In the gravity-free case, the equilibrium crystal shape (ECS) is characterized by a *scale invariance*. The presence of gravity breaks the scale invariance and the resulting ECS changes as the volume of the crystal  $V$  is changed. Moreover, the presence of gravity breaks the translational invariance along the direction it acts. Physically realized by the necessity of a support, this is manifested by the existence of an *inhomogeneous effective pressure*  $P_{\text{eff}}$ , which divides the space into two regions, with  $P_{\text{eff}}$  either negative or positive. The ECS changes as the crystal passes from one region to another, being *concave* where  $P_{\text{eff}} < 0$ , and *convex* where  $P_{\text{eff}} > 0$ .

In all cases it was possible to express the corresponding ECS in terms of the gravity-free one.

For the hung crystal, i.e., a crystal pinned to a vertical wall at the top, it is shown that some orientations are *missing* from the ECS that otherwise will be present in the gravity-free ECS, adsorbed on the same substrate. Thus, facets could disappear from the crystal shape as the vo-

CSL 1/13/89

lume  $V$  or the gravitational acceleration  $g$  is increased. A critical volume  $V_c$  is found, so that if the crystal volume  $V$  exceeds  $V_c$ , the crystal cannot be pinned. The ECS can exhibit both concave and convex portions.

For a crystal, pinned to a vertical wall at its lower end, we find that it will never develop a concave part. On the other hand, *new orientations*, absent from the gravity-free crystal, will be present on its ECS.

The ES of a free and pinned crystal meniscus is also solved and an expression for the excess (depleted) volume  $\Delta V$  is derived. The solution for the crystal meniscus between two walls is also presented.

For the pendant crystal, i.e., a crystal hanging from a horizontal support, we find that it can exhibit both concave and convex portions on its ECS. When it develops a concave part, *new orientations* will appear, compared to the gravity-free case. An intuitive stability criterion is introduced, according to which only crystals wetting the substrate can develop a concave portion before they break.

The treatment of a crystal on an inclined substrate shows the complications that arise in determining the ES for a general position of the support as a result of the conflict between the directions associated with gravity and support.

An expression for the facet length in the presence of gravity is obtained that is valid for all types of support. For crystal shapes that display a concave portion it offers a very convenient way to experimentally measure step free energies. Thus, by breaking scale invariance, the presence of gravity allows absolute measures of surface energy in contrast to the gravity-free case, where the facet length is proportional to the step free energy by an unknown scale.

## ACKNOWLEDGEMENTS

I would like to express my deep gratitude to my advisor Dr. R. Zia for his guidance, *patience* and support during the course of this work and the preparation of this manuscript.

Thanks are also extended to the members of my committee for their time and helpful comments, as well as my fellow graduate students for their friendliness and encouragement.

## CONTENTS

Chapter 1	Introduction	1
Chapter 2	Preliminaries	5
2.1	Thermodynamic definition of surface tension	5
2.2	Laplace formula	11
2.3	Surface tension of crystals and the polar $\gamma$ -plot	13
2.4	The equilibrium shape of crystals and the Wulff construction	15
2.4.1	The Wulff construction	17
2.4.2	Parametric solution of the equilibrium crystal shape	19
2.4.3	Analytical approach	21
2.4.4	Effect of substrates on the equilibrium crystal shape - the Winterbottom construction	23
2.4.5	Andreev's relation	26
2.5	Chemical potential of the equilibrium crystal shape - the effect of curvature	29
2.6	Corner points on crystal surfaces	31
Chapter 3	Equilibrium shape of a crystal adsorbed to a wall	34
3.1	Crystal pinned at top	35
3.1.1	The variational problem	35
3.1.2	Equilibrium shape of a crystal pinned at top	37
3.1.3	Results	43
3.2	Crystal pinned at bottom	49

3.3	Equilibrium shape of a free and pinned meniscus	51
Chapter 4	Equilibrium shape of a pendant crystal	64
Chapter 5	Equilibrium shape of a crystal on an inclined plane	73
Chapter 6	Summary and outlook	80
References		84
Figures		88
Curriculum Vitae		102

LIST OF FIGURES

- Fig. 1. A two-dimensional simple cubic crystal lattice. The broken line represents a crystal surface with indices (16) and an angle of inclination to the base (horizontal) face (01)  $\theta$ , where  $\theta = \tan^{-1}(1/6)$ . 88
- Fig. 2. The Wulff construction in two dimensions. Through point A on the  $\gamma$ -plot with a radius vector  $OA = \gamma(n)n$  from the origin O draw a line (plane) BC normal to  $n$ . The inner envelope of planes like BC, normal to the radii of the  $\gamma$ -plot  $\Gamma$ , gives the equilibrium crystal shape. Note that point M on the crystal surface has surface energy corresponding to point A on the  $\gamma$ -plot. 89
- Fig. 3. Geometrical illustration of the derivation of the Wulff construction in two dimensions. A straight line  $\alpha$  with a fixed slope  $p_0$  that belongs to the family (2.21) is drawn. It makes an angle  $\phi_0 = \tan^{-1}(p_0)$  with the positive x-axis and has an intercept  $b = h(p_0)/\lambda$  with the y-axis. OD is the distance from the origin O to the straight line and it is equal to  $[h(p_0)/\lambda]\cos(\phi_0) = \gamma(p_0)/\lambda$ . This shows that the distance from the origin to any straight line of the family (2.21), which has as its envelope the ECS, is proportional to  $\gamma(p)$  and that is the Wulff construction. OM is the distance from the origin to the point M of the crystal surface given by  $OM = OD/\sin(\theta - \phi_0)$ . 90
- Fig. 4. Geometric construction for the analytic solution. The ECS is given in polar coordinates  $(r, \theta)$ .  $\psi$  is the angle the normal  $n$  makes with the positive x-axis. From the figure follows the dependence of the angle  $\psi$  on  $r(\theta)$ , given by  $\tan(\theta - \psi) = dr/rd\theta$  (after [46]). 91
- Fig. 5. Wulff-Winterbottom construction for  $\gamma_{\Delta} < 0$  in two dimensions for an ECS given by  $y = y(x)$ , with the contact angles  $\phi_0$  and  $\phi_f$  identified. For a faceted crystal the contact angles can not be related to a unique value of  $\gamma_{\Delta}$ . 92
- Fig. 6. Geometrical relation between  $G(T, H)$  and  $F(T, M)$  for a ferromagnet at a fixed temperature  $T < T_c$  (after [45, 50]).  $H$  is the magnetic field,  $M$  is the magnetization obtained from  $G(T, H)$  by  $M = -(\partial G/\partial H)_T$  and  $T_c$  is the Curie temperature. The tangent to the curve  $G(H)$  at point  $(H, G(H))$  in-

tercepts the  $H = 0$  axis at a height  $F$ , so that  $(F - G)/H = -(\partial G/\partial H)_T = M$  and we obtain the Legendre transformation between  $F(T, M)$  and  $G(T, H)$ . The point to note is that the cusp of  $G(H)$  at  $H = 0$  leads to a region of magnetizations between  $[-M_0, M_0]$  for which  $F(M)$  is not defined. The drawing of the figure utilizes the fact that  $G(T, H)$  is a concave function of the magnetic field  $H$  and  $F(T, M)$  is a convex and even function of the magnetization  $M$  [50].

93

Fig. 7. Crystal pinned at top to a wall in the presence of a gravitational field. The point the crystal is pinned to the wall is taken as the origin of the coordinate system. The position of the wall (substrate) is given by  $x = 0$ . The angles  $\omega_p$  and  $\omega_f$  are the angles the tangent to the ECS makes at the support (pinning) point and at the free end of the crystal with the positive  $y$ -axis. The gravitational force is directed along the positive  $y$ -axis.

94

Fig. 8. Wulff-Winterbottom diagram for  $\gamma_\Delta < 0$  in two dimensions for an equilibrium crystal shape given by  $x = x(y)$ , with the contact angles  $\omega_p, \omega_f$  identified. The points  $P$  and  $P^*$  on the Wulff shape have tangents which make angles  $\omega_p$  and  $\omega^*$  with the positive  $y$ -axis.

95

Fig. 9. Crystal pinned at bottom to a wall in the presence of a gravitational field. The case is mathematically identical to that depicted in Fig. 7., but with the direction of the gravitational field reversed. The point of pinning is chosen as the origin  $O$  of the coordinate system and  $\omega_p$  and  $\omega_f$  are the contact angles at the point of support  $P$  and at the free end of the crystal. The end of the crystal  $y(\phi_f)$  is positive ( $y(\phi_f) > 0$ ).

96

Fig. 10. Meniscus of a semi-infinite crystal or fluid bounded by a vertical plane wall at  $x = 0$  for  $\gamma_\Delta < 0$ .  $\omega_0$  is the contact angle of the meniscus with the vertical wall and  $y_0$  is the rise of the wetting meniscus at the wall. Note that the contact point of the meniscus with the wall is taken as the origin of the coordinate system.

97

Fig. 11. Wetting ( $\gamma_\Delta < 0$ ) semi-infinite crystal menisci separated by a vertical plane wall with both sides the same placed at  $x = 0$ .  $\omega_0$  ( $\omega'$ ) is the contact angle with the vertical wall and  $y_0$  ( $y'$ ) is the rise at the wall of the meniscus that extends into the  $x > 0$  ( $x < 0$ ) region.

97



Fig. 12. Wulff-Winterbottom diagram illustrating the determination of the contact angles  $\omega$  and  $\omega'$  of the two semi-infinite menisci, separated by a vertical wall.  $m$  is the fixed orientation of the wall with respect to the semi-infinite interface that extends into the  $x > 0$  region ( $m = -x$ , where  $x$  is the unit vector in the positive  $x$ -direction) and  $m'$  is the fixed orientation of the wall with respect to the meniscus that lies in the  $x < 0$  region. The points  $P$  and  $P'$  on the Wulff-Winterbottom shape have tangents, which make angles  $\omega$  and  $\omega'$  with the positive  $y$ -axis. The new orientations, both menisci exhibit when compared to the gravity-free ECS on the same substrate, correspond to the angles the tangents at all points of the portion  $PAP'$  of the Wulff-Winterbottom shape make with the positive  $y$ -axis.

Fig. 13. Two-dimensional wetting meniscus of a crystal between two parallel vertical plane walls.  $\omega$  and  $\omega'$  are the contact angles of the meniscus with the left and right wall with respect to the positive  $y'$ -axis,  $h$  is the meniscus rise between the walls,  $y_0$  is the rise of the semi-infinite meniscus at the right wall and  $\epsilon$  is the difference of the  $y$ -coordinates of the points  $O$  and  $O'$ , where  $O$  is the point of contact of the semi-infinite meniscus with the right wall and  $O'$  is the origin of the coordinate system. Note also that in general, the points of contact  $O'$  and  $O_1$  of the meniscus between the walls with the left and right wall respectively do not have the same  $y$ -coordinate. The same is also true for the points of contact  $O$  and  $O_2$  of the semi-infinite menisci with the right and left wall respectively. This difference between the  $y$ -coordinates of the two pairs of contact points is due to the asymmetry of the  $\gamma$ -plot, as explained in the text. The separation between the walls is  $s$ .

Fig. 14. Crystal hanging from a horizontal support in the presence of a gravitational field (the pendant crystal).  $\phi_0$  and  $\phi_1$  are the contact angles of the pendant crystal at the origin and at the right end respectively, with the positive  $x$ -axis. Gravity is directed along the positive  $y$ -axis.

Fig. 15. Crystal supported on an inclined plane in the presence of a gravitational field.  $\omega$  and  $\omega_f$  are the angles the tangent to the equilibrium crystal shape makes with the positive  $y$ -axis at the point of pinning and at the free end respectively.  $\alpha$  is the angle the tangent to the ECS makes with the positive  $Y$ -axis and  $\theta$  is the angle between the positive directions of the  $y$ -axis and the  $Y$ -axis. The gravitational field is along the positive  $y$ -axis.

## CHAPTER 1

### INTRODUCTION

Recent experiments on  $^4\text{He}$  and small (micron-size) metallic crystals in thermal equilibrium with the surrounding phase [1-10] have initiated a considerable theoretical interest [11-15] towards the century-old subject of equilibrium crystal shapes [16-20], i.e., shapes that minimize the free energy of the system, subject to a constant volume constraint.

In these experiments thermal equilibrium is supposedly achieved, so that the resulting equilibrium crystal shape (ECS) is determined by thermodynamic considerations only. Different facets of the equilibrium crystal shape are used to experimentally test current theoretical concepts of phase transitions of surfaces. A notable example is the roughening transition which is associated with morphological changes in the equilibrium crystal shape - the disappearance and reappearance of certain facets of the equilibrium shape (ES) as the temperature is raised or lowered.

Since the dimensions of the  $^4\text{He}$  crystals used were large (5-9 mm) compared to the capillary length (1.4 mm for hcp  $^4\text{He}$ ), it is expected that gravity will play a role in the determination of the equilibrium shape. So, an understanding of the effects of gravity on the equilibrium crystal shapes is required in order to obtain a correct interpretation of the experimental results. One of the questions that naturally arises in connection with roughening is: can the presence of gravity lead to the appearance or disappearance of some facets that will otherwise be absent or present in the gravity-free equilibrium shape, or stated differently,

does the equilibrium shape of the crystal depend on its volume  $V$ . The observation made in [4] that the types of facets that appear on the hcp <sup>4</sup>He crystals pinned to a wall depend, among other things, on the crystal size too, is particularly interesting, since in the gravity-free case the equilibrium shape of a crystal is independent of its size [11-20]. Thus, gravity appears to play a role in the equilibrium crystal shapes in these experiments [1-4].

When gravity is introduced, the scale invariance is lost and the volume would affect the equilibrium crystal shape [15]. A way to understand this is to note that we cannot form a length parameter from  $\gamma$  (specific surface free energy, or surface tension, to be defined below) alone against which the volume of the crystal  $V$  can be measured. However, when gravity is present, a characteristic length is introduced - the capillary length  $\alpha = (2\gamma/\rho g)^{1/2}$ , where  $\rho$  is the difference in density between the crystal and the medium,  $\rho = \rho_c - \rho_m$ , and  $g$  is the gravitational acceleration. Compared to this length, the effects of the volume (size) of the crystal can be felt.

As discussed in [15,21], in order to obtain the equilibrium crystal shape in the presence of gravity, some kind of boundary conditions must be imposed. So, we have to specify the way the object is supported in order to find a minimum of the free energy functional. Otherwise, no minimum of the energy functional exists. Part of the difficulty encountered with the effects of gravity on equilibrium shapes is the strong dependence of solutions on the details of the supports. This is a common experience, especially for cases where the surface free energy per unit area  $\gamma$  of the interface between the two media is isotropic: water

droplets on tables are shaped differently from those hanging from faucets. For isotropic  $\gamma$ , a large variety of situations have been explored [22-25] in both two and three dimensions.

The case of interest in the present study is anisotropic  $\gamma$ , which is characteristic of crystals (the origin or the physical reasons for the anisotropy of the surface tension of crystals will be discussed in Chapter 2). For general  $\gamma$ , only a few address the problem of gravity in the treatment of equilibrium shapes. Cabrera and Garcia [26] evaded the issue essentially. Avron et al. [21] considered sessile drops, i.e., crystals supported by a homogeneous, flat horizontal surface such as tabletop. For an arbitrary given  $\gamma$ , exact solutions (quadrature) are found in two dimensions, while general properties are proved in all higher dimensions. The effect of gravitational induced faceting was discovered and extended by Taylor [27] to gravitational induced curvature. Another group [28] studied a crystal-medium interface inside a cylindrical volume with arbitrarily shaped normal section and managed to obtain an expression for the sizes of plane strips on the interface.

Quite recently, Avron and Zia [29] obtained a fascinating result which showed that gravity can transmute a surface critical exponent, associated with the so-called "vicinal surfaces", which are rounded portions of a crystal surface near a facet direction. The approach of the vicinal surfaces to the facet may be described by the equation  $\eta \sim \xi^n$ , where  $\eta$  is the deviation of the vicinal surface from the extrapolation of the facet plane,  $\xi$  is the distance from the facet edge and  $n$  is the exponent. The main result of [29] is that when gravity acts on a horizontal facet, for sufficiently large crystals, the exponent  $n$  can be changed

to  $n/(2 - n)$ . In particular,  $n = 3/2$  is the value recent theories predict for the gravity-free case. An excellent agreement was found when the results of [30] were reanalysed with the transmuted power of  $n = 3$ .

Motivated by experiments on large hcp  ${}^4\text{He}$  crystals [1-4], we study the effects of gravity on equilibrium crystal shapes. Three different types of support are considered - the hanging crystal (vertical support), the pendant crystal and a crystal on an inclined plane. Their effect on the equilibrium crystal shape in the presence of gravity in two dimensions is analyzed. For arbitrary  $\gamma$ , we obtain explicit expressions for the equilibrium crystal shape in terms of the gravity-free shape.

At this time, an experimental analogue of a two-dimensional crystal does not exist to compare with these calculations. But in the future it may be possible to grow crystals in a chamber where one dimension of the crystal is much smaller than the length of a facet, so that a two-dimensional model may reasonably apply.

Throughout the present work, we consider the surface tension  $\gamma$  to be given as a function of the orientation  $n$  of the interface and not to depend on the gravitational field.

## CHAPTER 2

### PRELIMINARIES

In this Chapter we introduce and define the basic concepts that are essential for the presentation and discussion of the results obtained in the present work. In all of the subsequent exposition the general results will be illustrated for the two-dimensional case, because of its simplicity. Another important reason is the existence of analytic solutions for some cases that consider gravity (see [21] and §§3-5 below) in 2-d.

#### 2.1. Thermodynamic Definition of Surface Tension [31-35,18,19,14]

When a system consists of two homogeneous phases 1 and 2 in contact, there exists a (narrow) transitional layer (interface) which separates the two bulk phases and within which the values of the extensive thermodynamic parameters change as we cross this layer.

If we denote by  $A$  the area of the interface and if we consider a process where this area undergoes an infinitesimal reversible change  $dA$ , then the work done in changing the area is proportional to  $dA$  and can be expressed as

$$\gamma dA \tag{2.1}$$

where  $\gamma$  is called the surface tension. A function of the state of the whole system,  $\gamma$  is positive. If the surface tension were negative ( $\gamma < 0$ ),

the interface between the two phases would tend to increase without limit and the two phases would at the end mix.

The total work  $dW$  includes both the work done by the homogeneous bulk phases ( $- P^k dV^k$ ,  $k = 1, 2$ ) and the work necessary to change the surface

$$dW = - P^1 dV^1 - P^2 dV^2 + \gamma dA \quad (2.2)$$

Here we note that we are considering only volume work and the amount of work is positive when the work is done on the system by external forces. In this case the volume work is  $- PdV$ .

For a system in thermodynamic equilibrium, the energy balance is expressed by

$$dU = TdS + dW + \sum_{i=1}^m \mu_i dN_i \quad (2.3)$$

where  $U$  is the internal energy,  $m$  is the total number of components (i.e. distinguishable species),  $\mu_i$  is the chemical potential of component  $i$ , which is the same in the whole system,  $N_i$  is the number of moles of the  $i$ -th species,  $T$  is the absolute temperature and  $S$  is the entropy.

In what follows, we will restrict the treatment to one-component ( $m = 1$ ) two-phase system. At the end of this section we will state some results for the general case of a multi-component system.

Using eq.(2.3), the expression for the differential of the internal energy  $dU$  becomes

$$dU = TdS - P^1 dV^1 - P^2 dV^2 + \gamma dA + \mu dN \quad (2.4)$$

Since  $U$  is a homogeneous function of first degree, by the Euler theorem we get

$$U = TS - P^1 V^1 - P^2 V^2 + \gamma A + \mu N \quad (2.5)$$

In the treatment of interfaces it turns out to be more convenient to use as the fundamental thermodynamic potential  $\Omega$ , defined by

$$\Omega = F - \mu N = U - TS - \mu N \quad (2.6)$$

where  $F$  is the Helmholtz free energy.

From eqs. (2.5) and (2.6) we get an explicit expression for  $\Omega$

$$\Omega = - P^1 V^1 - P^2 V^2 + \gamma A \quad (2.7)$$

and for the differential  $d\Omega$  we obtain

$$d\Omega = - SdT - P^1 dV^1 - P^2 dV^2 - Nd\mu + \gamma dA \quad (m = 1) \quad (2.8)$$

where we have used eqs.(2.4) and (2.6).

From eq.(2.8) we see that  $\Omega$  depends on the independent variables  $T$  and  $\mu$  (and the volume  $V$ , since  $\Omega$  is an extensive quantity). The convenience of  $\Omega$  is due to the fact that the temperature  $T$  and the chemical potential  $\mu$  have equal value in the two phases at thermodynamic equilibrium, while the pressures  $P^1$  and  $P^2$  are not in general equal when surface



effects are taken into account.

Gibbs [31] was first to realize that in applying the thermodynamic approach to multi-phase systems, it is convenient to associate definite amount of extensive thermodynamic quantities (energy, entropy, etc.) with a given area of "surface". In this way, any extensive thermodynamic quantity of the system  $X$  can be written as a sum of "volume" parts and a "surface" part

$$X = X^1 + X^2 + X^S \quad (2.9)$$

This division is not unique, since the transition layer separating the two phases has to be replaced by a geometrically constructed dividing surface to which we attribute all the properties and effects which arise from the existence of the physical interface (in other words, we ignore how the extensive thermodynamic quantity  $X$  interpolates between the bulk values  $X^1$  and  $X^2$  far from the interface). Moreover, the decomposition (2.9) assumes that both bulk phases 1 and 2 retain their properties up to the dividing surface, which is called the Gibbs surface and whose location is usually chosen according to a certain convention which needs to be specified.

At this point it is appropriate to mention that in general the quantities  $X^1$ ,  $X^2$  and  $X^S$  will depend on the location of the Gibbs surface. So, in general it will not be possible to assign to the surface quantities (to the  $X^S$ 's) real physical properties of the system, unless these surface quantities or some combinations of them are invariant with respect to the location of the dividing surface and consequently can be re-

lated to experimental measurements.

For the one-component two-phase system which we are considering, the location of the dividing surface can be made unique by demanding that

$$V = V^1 + V^2 \quad \text{and} \quad N = n^1 V^1 + n^2 V^2 \quad (2.10)$$

where  $V$  is the total volume of the system,  $N$  is the total number of moles in the system and  $n^k$  ( $k = 1, 2$ ) =  $n^k(\mu, T)$  are the number of moles per unit volume in each phase. In this case  $N^S = 0$ .

Eqs.(2.10) determine the choice of the volumes  $V^1, V^2$ , the number of moles  $N^1, N^2$  and hence the volume parts of all thermodynamic quantities. From eq.(2.7) we have that  $\Omega^S = \gamma A$  and since  $F = \Omega + N\mu$  and  $N^S = 0$ , we obtain for the surface free energy  $F^S$  that

$$F^S = \gamma A \quad (2.11)$$

Eq. (2.11) shows that in a one-component two-phase system when the convention for the location of the dividing surface is chosen according to eqs. (2.10), the surface tension  $\gamma$  is equal to the specific surface free energy or Helmholtz free energy per unit area ( $\gamma = F^S/A = f^S$ ).

So, from macroscopic point of view, eq. (2.1) can be considered the thermodynamic definition of the surface tension  $\gamma$ . This shows that  $\gamma$  has the meaning of a (mechanical) energy which is necessary to create a new surface. In this case  $\gamma$  depends on the location of the Gibbs dividing surface. For planar interfaces though (where  $P^1 = P^2$ ), the surface tension  $\gamma$  is an invariant, since in this case  $\Omega = -PV + \gamma A$  (see eq.(2.7)) and  $\Omega$ ,

$P$ ,  $V$  and  $A$  are invariant with respect to the location of the Gibbs dividing surface.

In the general case involving  $m$  components (i.e., distinguishable species), we have

$$\gamma = f^S - \sum_{i=1}^m \mu_i \sigma_i$$

where  $\sigma_i = N_i^S/A$  is the surface density of the  $i$ -th component in the system. This shows that the surface tension  $\gamma$  cannot be identified with the specific surface free energy. If the dividing surface is chosen so that  $\sum_{i=1}^m \mu_i N_i^S = 0$  (summation convention used), only then the surface tension  $\gamma$  reduces to  $f^S$ .

Although the above discussion of the surface tension may seem rather long, we would like to mention that it is important to correctly define the thermodynamic variables that control the state of the surface and that are used to define the equilibrium crystal shape. Very nice expositions that treat the subject of surface thermodynamics of solids (except that of Gibbs [31]), which have appeared more recently, are those of J. W. Cahn and R. B. Griffiths [32,33].

Quite recently a number of papers appeared that treat the interplay between elastic surface stress and surface energy [36-39], first pointed out by Herring [18]. Without going into any discussion of the relation between surface stress and surface tension, it should be mentioned that the relevant physical quantity to be used when treating equilibrium crystal shapes is the surface tension  $\gamma$ , as defined above.

As a final remark to this section we point out that the dependence

of the surface tension  $\gamma$  on the curvature of the surface will not be taken into account during the subsequent exposition. This dependence is negligible if the radius of curvature of the surface is large compared with the thickness of the physical interface (which has dimensions on the atomic scale). For the same reason we also neglect the inhomogeneous volume stresses induced by the presence of the surface, which are inversely proportional to the linear dimensions of the crystal or to its local radii of curvature [18].

## 2.2. Laplace Formula [35,40]

The existence of a curved interface between two phases leads to a difference in the pressures of the two phases, which is called a surface pressure. This difference in pressure can be determined from the condition of mechanical equilibrium, i.e. the sum of the forces acting on each phase at the interface should be zero. This sum is given by the derivative of a thermodynamic potential with respect to the displacement of the interface, the other variables, corresponding to this potential are held constant.

If we consider two *isotropic* phases (two liquids or a liquid and a vapour) and assume that phase 1 is a sphere of radius  $r$  imbedded in phase 2, then the pressure is constant within each phase and the potential  $\Omega$  is given by eq.(2.7). The pressure of the two phases satisfy the relation  $\mu^1(P^1, T) = \mu^2(P^2, T) = \mu$ , where  $\mu$  is the common value of the chemical potential in the two phases (the superscripts denote the phase; recall also that we are considering a one-component two-phase system). Hence, for

constant  $\mu$  and  $T$  we must regard  $P^1$  and  $P^2$  as constants. The same applies for  $\gamma$  too, since  $\mu$  and  $T$  specify the state of the system and as it has already been mentioned before,  $\gamma$  depends on the state of the system. The condition for mechanical equilibrium (for constant total volume of the system  $V = V^1 + V^2$ ,  $\mu$  and  $T$ ) is obtained from eq.(2.7) by differentiating  $\Omega$  with respect to  $r$  (i.e. the displacement of the interface)

$$(\partial\Omega/\partial r)_{V,T,\mu} = - (P^1 - P^2)dV^1/dr + \gamma dA/dr = 0 \quad (2.12)$$

and using  $V^1 = 4\pi r^3/3$  and  $A = 4\pi r^2$  we arrive at

$$P^1 - P^2 = 2\gamma/r \quad (2.13)$$

which is the famous Laplace formula (equation). For a planar interface ( $r \rightarrow \infty$ ), the bulk phases have the same pressure.

In the general case, when the surface of separation of the two phases is curved (but not a sphere as it was assumed in the above example), the expression for the pressure difference of the two *isotropic* phases takes the form [40]

$$P^1 - P^2 = \gamma(K_1 + K_2) \quad (2.14)$$

where  $K_1$  and  $K_2$  are the curvatures of the principal sections through a given point of the interface. The sign of  $K_i$  in this equation means that the pressure is greater in the phase, occupying a convex region.

### 2.3. Surface Tension of Crystals and the Polar $\gamma$ -plot [14,18,19,41,35]

Up to this point we considered the surface tension of surfaces separating two isotropic phases. The surface tension of an interface between two phases, at least one of which is anisotropic (i.e., a crystal), depends on the orientation of the crystal surface with respect to the crystallographic axes.

The most convenient way to display the anisotropy of  $\gamma$  is the polar diagram. This is a closed surface, the radii of which from a fixed origin are  $\Gamma = \gamma(n)n$ , where  $n$  is the unit vector, outwardly normal to a given crystal surface, and  $\gamma(n)$  is the corresponding surface tension. It is clear, that the magnitude of  $\Gamma$  in any particular direction is equal to the value of  $\gamma$  for the surface normal to  $\Gamma$ .

At this point a few words are in order about the physical origin of the orientation dependence of the interfacial free energy. Consider a crystal co-existing with a fluid. A crystal is a *periodic* system, while the fluid is *homogeneous*. Because of the *breaking of spherical symmetry* in the solid, the surface energy at the crystal-fluid boundary is a specific function of the surface orientation, as shown by Landau [41].

Some characteristic features of the  $\gamma$ -plot are best exhibited by considering a two-dimensional (2-d) example - a simple cubic crystal lattice (a square grid) at  $T = 0^\circ$  K. The crystal planes are represented by straight lines through the lattice points - see Fig. 1. Following Landau [41], let us consider the surface tension of a crystal surface that is inclined at a small angle  $\theta$  to the (01) face with indices  $(1n)$ , where  $n$  is large. It is clear from Fig. 1. that any crystal surface

(i.e., a surface with rational indices) can be built up by an appropriate periodic sequence of spacings (terraces) between steps (ledges). Let  $\gamma_0$  be the surface tension of the (01) face (the terrace). The surface of the crystal bounded by the face (ln) consists of terraces of length n (in units of the lattice parameter a), which is large and ledges of height that is small compared to the terraces's length.

The presence of each ledge leads to the appearance of some additional surface energy  $\beta$  per unit length of an isolated ledge. When the interaction between steps may be neglected (i.e. when n is large or the inclination angle  $\theta$  is small, so that the steps are far apart) we can write the surface tension of an inclined surface  $\gamma$  as the sum of  $\gamma_0$  and the energy of the steps  $\beta/na$  per unit length (since the distance between steps is na, the number of steps per unit length is  $1/na$ ). If the angle  $\theta$  between the planes (ln) and (01) is used, then for sufficiently large n,  $\theta = 1/n$  and for the surface tension  $\gamma$  of the face (ln) we get

$$\gamma = \gamma_0 + \beta\theta/a, \theta > 0 \quad (2.15)$$

If  $\theta \rightarrow 0$ , i.e. n tends to infinity, the ratio  $(\gamma - \gamma_0)/\theta$  approaches a finite limit, which may be regarded as the derivative  $d\gamma/d\theta = \beta/a$ . If a surface with the same indices (ln) is inclined in the opposite direction to the face (10), applying the same argument as above gives  $\beta/na$  for the change in surface tension of the inclined surface. But now  $\theta = -1/n$ , so that  $\gamma = \gamma_0 - \beta\theta/a$  and the derivative  $d\gamma/d\theta = -\beta/a$ .

At this point we see a very important feature of the surface tension of a crystal. Namely, that the surface tension of a crystal face may be

written as a continuous function of the direction of the face (i.e. angle  $\theta$ ) with respect to a certain orientation. Moreover, the derivative of the surface tension with respect to the angle  $\theta$  has at  $\theta = 0$  a finite jump, which for the above example is equal to  $2\beta/a$ . The difference  $\Delta(d\gamma/d\theta)$  between the two values of the derivative with respect to a given crystallographic orientation is a very important characteristic of this function.

Even from the above simple model we see the most general features of the surface tension: i) the dependence of the surface tension on the crystallographic orientation of the surface, i.e. the *anisotropy* of  $\gamma$  and ii) the appearance of cusps at particular orientations of the  $\gamma$ -plot, (i.e. orientations, corresponding to close-packed surfaces) where the derivative of the surface tension  $d\gamma/d\theta$  is discontinuous.

At higher temperatures, the shape of the  $\gamma$ -plot changes, and in certain cases the cusps disappear before the melting point of the crystal is reached. We will not discuss this problem further. A nice review that discusses this topic is that by C. Rottman and M. Wortis [14].

#### 2.4. The Equilibrium Shape of Crystals and the Wulff Construction

From the knowledge of the surface tension as a function of orientation, it is possible to determine the equilibrium crystal shape. The equilibrium shape of a crystal (or an interface) is determined by the condition for the thermodynamic potential  $\Omega$  to be a minimum for given temperature  $T$ , chemical potential  $\mu$  and volume  $V$  of the crystal. Equivalently, its surface part to be a minimum,



$$\Omega^S = \oint \gamma dA = \min, \quad (2.16)$$

the integral being taken over the whole surface of the crystal subject to a volume constraint. Since we are considering a one-component two-phase system for which the specific free energy  $f^S$  is equal to the surface tension  $\gamma$ , the condition (2.16) is also a condition for the surface free energy  $F^S$ .

For our 2-d case we can use a "left-handed" coordinate system  $(x,y)$  in the plane of the crystal, where  $y(x)$  will be the equation of the crystal shape. The function  $y(x)$  is determined from condition (2.16), which in 2-d is the same as finding the minimum value of the line integral  $\oint \gamma ds$  (where  $ds$  is the line element  $ds = (1 + p^2)^{1/2} dx$  and  $p = dy/dx$ ) for a fixed area  $\int y dx$ . It should be noted that the direction of the tangent is the same as the direction of the curve (line), which is positive when traversed anticlockwise. Since the surface tension  $\gamma$  depends on the orientation of the crystal face  $n$ , which, in 2-d can be specified by the angle  $\psi$  it makes with the positive direction of the  $x$ -axis,  $x$  ( $\psi = \cos^{-1}(n \cdot x)$ ). Alternatively,  $\gamma$  can be parametrized by the direction of the tangent to the required curve, i.e.  $\gamma = \gamma(p)$ . The problem of finding the minimum of the free energy functional  $F[y]$ , with the volume of the crystal being constant, reduces to finding the extremum of

$$F[y] - \lambda V = \int [\gamma(p)(1 + p^2)^{1/2} - \lambda y] dx = \int [h(p) - \lambda y] dx \quad (2.17)$$

where  $\lambda$  is the Lagrange multiplier connected with the constant volume constraint and  $h(p) = \gamma(p)(1 + p^2)^{1/2}$ .

### 2.4.1. The Wulff Construction [14-19,35]

The general relationship between the polar diagram of the surface tension and the ECS is called the Wulff theorem or Wulff construction, which consists of the following. Given the  $\gamma$ -plot, the ECS is to be found as the inner envelope of planes normal to the radii of the  $\gamma$ -plot  $\Gamma$  - see Fig. 2. In what follows, we will give a proof of the Wulff construction in 2-d, following the approach of L. D. Landau and E. M. Lifshitz [35].

The Euler-Lagrange equation for the variational problem (2.17) leads to

$$d(\partial h/\partial p)/dx = -\lambda \quad (2.18)$$

Since  $dy = p dx$ , we construct the Legendre transform of the crystal shape  $\zeta = px - y$  and we obtain that  $d\zeta = x dp$  (with  $x = d\zeta/dp$ ). It is easily seen that eq.(2.18) has an integral

$$h = -\lambda\zeta \quad (2.19)$$

and

$$y = (-pdh/dp + h)/\lambda \quad (2.20)$$

Eq.(2.20) is just the envelope of the family of straight lines

$$\Xi = y - px - h/\lambda = 0 \quad (2.21)$$

where  $p$  is a parameter. The above statement is verified if we recall that given a family of straight lines with one parameter  $\Xi(x,y,p) = 0$ , the envelope to the above family is determined by the following conditions - (a)  $\partial\Xi/\partial p = 0$  and (b)  $\Xi = 0$ . In our case, (a) leads to  $x + (\partial h/\partial p)/\lambda = 0$  and if we substitute for  $x$  in eq.(2.21) we get eq.(2.20).

Here we have to note that the envelope curve (2.20) is tangent to the family of straight lines (2.21) only at one point. This can be seen as follows. If we fix the value of  $p = p_0$  we get a certain straight line,  $l_0$ , belonging to the family (2.21). If we now use the same value of  $p$  in conditions (a) and (b) (that determine the envelope), we get a point  $M_0(x_0, y_0)$  where the envelope is tangent to the line  $l_0$  and since we have two equations in two unknowns, the point  $M_0$  is only one (if it exists).

Now, it is clear that the result obtained from the solution of the variational problem (eqs.(2.19) and (2.20)), expressed geometrically, is nothing else but the Wulff construction in 2-d. Eq.(2.21) describes a family of straight lines with a slope  $p$  and an intercept  $h/\lambda$ . If we fix  $p$ ,  $p = p_0$ , we will obtain a straight line which makes an angle  $\phi_0 = \tan^{-1} p_0$  with the positive  $x$ -axis and has an intercept  $h(p_0)/\lambda$  with the  $y$ -axis - see Fig. 3. The distance from the origin of the coordinate system to this line, denoted by  $OD$ , is given by  $OD = [h(p_0)/\lambda]\cos(\phi_0)$ . If we recall that  $h(p) = \gamma(p)(1 + p^2)^{1/2} = \gamma(p)/\cos(\phi)$ , we get that  $OD = \gamma(p_0)/\lambda$ . So, the distance from the origin to any straight line of the family (2.21), parametrized by the slope  $p$ , which has as its envelope the equilibrium shape, is proportional to  $\gamma(p)$  and that is the Wulff construction.

It should also be mentioned that the Wulff construction gives an equilibrium crystal shape that is convex. A proof for the convexity of the ECS in 2-d was given by W. W. Mullins [43].

#### 2.4.2. Parametric Solution [41,15]

The analytic solution of the equilibrium crystal shape, first obtained by L. D. Landau [41], is best given in parametric form. The Euler-Lagrange equation (2.18) can be integrated and the x- and y-coordinate of the equilibrium crystal shape are given by [41,15]

$$x = -[\gamma(\phi)\sin(\phi) + (d\gamma(\phi)/d\phi)\cos(\phi)]/\lambda = x_w/\lambda \quad (2.22a)$$

$$y = [\gamma(\phi)\cos(\phi) - (d\gamma(\phi)/d\phi)\sin(\phi)]/\lambda = y_w/\lambda \quad (2.22b)$$

where  $\phi = \tan^{-1}p$  and it takes values from 0 to  $2\pi$ ,  $x_w$  and  $y_w$  are the coordinates of the Wulff shape and they are defined by eqs.(2.22) when  $\lambda = 1$ .

If  $\gamma$  is discontinuous at some angle (direction)  $\phi_i$ , then it follows from eqs.(2.22) that a facet appears in the ECS (a line segment for the 2-d case) since for that particular direction the derivative  $d\gamma/d\phi$  has two different values and eqs.(2.22) determine two pairs of values for x and y, i.e. two different points  $M_1(x_1, y_1)$  and  $M_2(x_2, y_2)$ . Each pair of points defines the ends of a straight line segment of boundary at a given angle  $\phi_i$  with respect to the x-axis. The length of the segment is  $l = [(x_2 - x_1)^2 + (y_2 - y_1)^2]^{1/2}$  and using eqs.(2.22) it is given by

$$\ell = [(\frac{d\gamma}{d\phi})_2 - (\frac{d\gamma}{d\phi})_1]/\lambda = [\Delta(\frac{d\gamma}{d\phi})]/\lambda = \ell_w(\phi)/\lambda \quad (2.23)$$

It turns out that  $\ell$  is the upper bound (for details see [15]) of straight line segments in the ECS proportional to the discontinuity  $\Delta(d\gamma/d\phi)$ . This shows that cusps in the  $\gamma$ -plot lead (in fact *may* lead, as discussed in [15]) to finite flat faces in the ECS.

Since it is important for the subsequent exposition, it should be pointed out that the coordinates of the Wulff shape  $(x_w, y_w)$  are uniquely determined, once the surface tension  $\gamma$  is specified. Note also that the units of the Wulff coordinates are those of surface free energy  $\gamma$ , while the coordinates of the physical shape  $(x, y)$  are obtained from  $(x_w, y_w)$  by scaling with  $\lambda$  (see eqs.(2.22)), where  $\lambda$  is equal to  $(W/V)^{1/2}$  ( $W$  is the volume of the Wulff shape and  $V$  is the volume of the crystal). In this sense, the volume of the crystal scales the gravity-free ECS, as stated in the Introduction.

In §3. of the dissertation it will be convenient to consider the ECS as being given by  $x = x(y)$  and the orientation of the crystal surface at any point is parametrized by the angle  $\omega$  the tangent at that particular point makes with the  $y$ -axis ( $\omega = \tan^{-1}(dx/dy) = \tan^{-1}(q)$ ). Obviously, this is equivalent to the parametrization of the normal  $n$  of the crystal face in 2-d by the angle  $\psi$  the normal makes with the  $x$ -axis, both angles being equal. The expressions for the coordinates of the Wulff shape are

$$x_w = [\gamma(\omega)\cos(\omega) - (d\gamma(\omega)/d\omega)\sin(\omega)] \quad (2.22c)$$

$$y_w = -[\gamma(\omega)\sin(\omega) + (d\gamma(\omega)/d\omega)\cos(\omega)] \quad (2.22d)$$

Here we use again a "left-handed" coordinate system, but the direction of the curve  $x = x(y)$  is considered positive when traversed in clockwise direction and  $\phi = \omega + \pi/2$ .

A final comment on the parametric solution is that if  $\gamma$  is rapidly varying, the equilibrium curve (as given by eqs.(2.22)) may intersect itself. Then,  $r_w = (x_w^2 + y_w^2)^{1/2}$  may be a multivalued function of  $\phi$ . As it is discussed in detail in [15], the Wulff shape in this case is given by the smallest distance  $r_w$  and a corner shows up at the intersection point. The result of this is that some orientations will be missing from the crystal shape. We will touch upon this subject again, when Andreev's relation [44] is considered in §2.4.5.

### 2.4.3. Analytical Approach [15]

In this approach the surface tension  $\gamma$  is considered to depend on the angle  $\psi$  (the angle which the normal to the surface  $n$  makes with the positive x-axis, i.e.  $\psi = \cos^{-1}(n \cdot x)$  and recall that we are always working in 2-d). The equilibrium crystal shape is given by a function  $R(\theta)$  in polar coordinates  $(r, \theta)$ .

Although using the analytic approach [15,46] we are going to derive the Wulff construction once again, it allows us to see the problem from a different angle. First, any questions, connected with the multivaluedness of the ECS  $y(x)$  as used to derive the Wulff construction in §2.4.1., are eliminated (recall that the ECS in the absence of gravity has a convex shape and the function  $y(x)$ , that describes the ECS is necessarily a two-

valued function of  $x$ ). On the other hand, it makes clearer the connection that exists between the surface tension  $\gamma(\psi)$  and the ECS  $R(\theta)$  [46].

In polar coordinates, the energy functional (eq.(2.17)), which we need to extremize, takes the following form

$$\int_0^{2\pi} [\gamma(\psi)r/\cos(\theta-\psi) - \lambda r^2/2] d\theta \quad (2.24)$$

where the area element is  $r^2 d\theta/2$  and  $ds = (dr^2 + r^2 d\theta^2)^{1/2} = rd\theta/\cos(\theta-\psi)$ .

The crucial element here is to see the dependence of the angle  $\psi$  (i.e.  $n$ ) on  $r(\theta)$ , which is given by  $\tan(\theta-\psi) = dr/dr\theta$  (this is easily seen through the geometric construction in Fig. 4.). Thus,  $\gamma$  contains an implicit  $r$  dependence.

The solution to the variational problem (2.24) is given by

$$R(\theta) = \gamma(\psi_0)/\lambda \cos(\theta-\psi_0) \quad (2.25)$$

where  $\psi_0(\theta)$  is obtained from the equation

$$\tan(\theta-\psi_0) = (\partial\gamma/\partial\psi)/\gamma \quad (2.26)$$

The equivalence between the analytical method and the Wulff construction was shown by Zia [15,46]. Eq.(2.25) has the following geometrical interpretation - for each point  $R(\theta)$  on the crystal surface, the distance from the center of the crystal to the tangent plane at that point is proportional to  $\gamma(\psi)$ . In the language of §2.4.1. (see Fig. 3.),  $R(\theta) = OM$ ,  $OD = \gamma(\psi)$  and  $OM = OD/\cos(\psi-\theta)$ , so the two constructions are equivalent.

#### 2.4.4. The Effect of a Substrate on the ECS - the Winterbottom Construction [20,15,46]

As mentioned in the Introduction, the treatment of equilibrium crystal shapes in the presence of gravity requires the existence of some kind of support. The simplest kind of support is a flat, homogeneous substrate with orientation  $m$ , which is fixed with respect to the crystal axes. In what follows, we will consider the effect of this simplest kind of substrate on the ECS for the gravity-free case. There are other phenomena associated with the presence of a substrate, like wetting and drying, that will not concern us here.

In general, the equilibrium shape of a crystal on a substrate will reflect both the influence of the substrate and the anisotropy of the surface tension of the crystal. Winterbottom has shown [20] that under conditions of constant temperature, volume, chemical potential and fixed orientation of the crystal-substrate interface, the ECS is determined by minimizing the surface free energy (eq.(2.16)), but with a generalized surface tension  $\gamma^*(n)$  defined as:  $\gamma^*$  equals the surface tension of the crystal-medium interface ( $\gamma^* = \gamma_{cm}$ ) for all orientations  $n$ , except  $n = m$ , and  $\gamma^* = \gamma_{cs} - \gamma_{ms} = \gamma_{\Delta}$  for  $n = m$ , where  $\gamma_{cs}$  and  $\gamma_{ms}$  are the surface tensions for the crystal-substrate and medium-substrate interface.

So, if we are given  $\gamma(n)$ , the substrate is characterized completely by  $\gamma_{\Delta m}$ . Thus, for a homogeneous crystal-substrate interface with a fixed orientation, the problem of determining the equilibrium shape of a crystal on a substrate is transformed into the simpler problem of determining



the ES of a free crystal with surface tension  $\gamma^*$ , which has already been solved above, i.e. the Wulff construction.

Now, if we draw the polar plot of  $\gamma^*$  (i.e., the  $\gamma$ -plot, but in the direction  $m$ , which specifies the orientation of the fixed crystal-substrate interface we plot the value  $\Gamma = \gamma_{\Delta} m$ ) and perform the Wulff construction, we will obtain the ES of a crystal on that particular substrate, characterized by  $\gamma_{\Delta}$ . This generalization of the Wulff construction to the  $\gamma^*$ -plot is called the Winterbottom construction, which is in fact the Wulff construction, truncated by a plane normal to  $m$  at a distance  $\gamma_{\Delta}$  from the origin.

It should be noted, however, that  $\gamma_{\Delta}$ , being a difference, is not necessarily positive. So, in the direction  $m$ , negative  $\gamma^*$  values are possible. Depending on the value of  $\gamma_{\Delta}$  (it provides a measure of the binding between the crystal and substrate), several crystal-substrate configurations exist [20]: if  $\gamma_{\Delta} \geq \gamma_{cm}(m)$ , it is a non-wetting (or complete drying) configuration; if  $\gamma_{\Delta} > 0$  or  $\gamma_{\Delta} < 0$ , it is partial wetting and when  $\gamma_{\Delta} \leq -\gamma_{cm}(-m)$ , we have complete wetting.

For a more in depth discussion of the effects of more than one substrate on the ECS and some new interesting constructions, one should consult references [46,47].

One other important quantity when we consider the ES of a crystal, adsorbed on a substrate, are the *contact angles*. These are the angles between the tangent planes (in 2-d, lines) of the crystal-medium interface and the substrate at the contact points. When the adsorbed phase is *isotropic*, there is a unique contact angle  $\phi$ , determined by  $\gamma_{\Delta}$  through the Young-Dupre equation [48], i.e.,  $\gamma_{fm} \cos\phi = \gamma_{ms} - \gamma_{fs}$  (where f stands for

fluid). For crystals, the problem is more complicated. Of course, the contact angles may be read directly from the Winterbottom construction [46]. Having in mind that our main purpose is to study the effect of gravity on the ECS and that geometrical constructions like these described above are not easily generalized to problems involving gravity due to the loss of scale invariance, we will give an explicit derivation of the contact angle equation, as well as obtain in parametric form Winterbottom's result (which will be useful later).

To obtain the ES of a 2-d crystal on a substrate parametrically, we let the crystal lie in the  $y > 0$  half-space, with the origin at one end of the crystal. Now, the energy functional will contain a term  $\int \gamma_{\Delta} dx$  that will take into account the energy contribution due to the line of contact between the crystal and the substrate. The complete free energy functional that is to be minimized is given by

$$F[y] = \int \{ \theta(y) [\gamma(1 + p^2)^{1/2} + \gamma_{\Delta}] \} dx \quad (2.27)$$

where  $\theta = 1, 0$  for  $y \geq 0, y < 0$  and  $V = \int \theta(y) y dx = \text{const.}$

Using once again Lagrange's method of undetermined multipliers, the solution is the shape  $y(x)$  which extremizes  $F - \lambda V$ . After solving the Euler-Lagrange equation of the variational problem (2.27), the Winterbottom shape ( $\lambda = 1$ ), denoted by  $(x_{wb}, y_{wb})$  is expressed in terms of Wulff's by the following relations

$$x_{wb}(\phi) = x_w(\phi) - x_w(\phi_0) \quad (2.28a)$$

and

$$y_{wb}(\phi) = y_w(\phi) + \gamma_{\Delta} \quad (2.28b)$$

where  $\phi_o$  is the contact angle at the origin, satisfying  $y_w(\phi_o) = -\gamma_{\Delta}$  (see Fig. 5. for a  $\gamma_{\Delta} < 0$  case). For the isotropic case ( $\gamma = \text{const.}$ ) this reduces to the familiar contact angle equation  $\gamma \cos \phi = -\gamma_{\Delta}$  (see eq.(2.22b). The other contact angle, denoted by  $\phi_f$ , also satisfies the condition  $y_w = -\gamma_{\Delta}$ . The condition  $y_{wb} = 0$  determines the contact angles of a crystal on a substrate and as such it is called the generalized Young-Dupre equation. It should be noted, however, that in the case of a faceted crystal, the contact angle  $\phi$  cannot be related to a unique value of  $\gamma_{\Delta}$ , as observed in [20]. This can be easily seen from a Winterbottom construction that gives a faceted crystal.

When the crystal and medium lie in the  $x > 0$  half-space, the Winterbottom shape is given by

$$x_{wb}(w) = x_w(w) + \gamma_{\Delta} \quad (2.28c)$$

$$y_{wb}(w) = y_w(w) - y_w(w_o) \quad (2.28d)$$

where  $w_o$  is the contact angle at the origin, satisfying  $x_w(w_o) = -\gamma_{\Delta}$ . The other contact angle  $w_f$  also satisfies the condition  $x_w(w_f) = -\gamma_{\Delta}$ .

#### 2.4.5. Andreev's Relation [44,45]

The derivation of the ECS as described in §2.4.1. and [35] was known for a long time, especially the fact that the variational problem (2.17)

had a first integral given by eq.(2.19), i.e.,  $h = -\lambda\zeta$ , where  $\zeta$  was the Legendre transform of the crystal shape. So, it is very surprising that it took so many years to discover that the ECS can be also related to the Legendre transform of the free energy  $h$ . It was Andreev [43] who realized this and the reasoning (simplified for the 2-d case) goes as follows.

From eq.(2.19) and the fact that  $d\zeta = xdp$  (see §2.4.1.),  $h$  may be considered a function of  $p$ ,  $h = h(p)$ . If we denote by  $\eta$  the derivative  $dh/dp$ , we get that  $\eta = dh/dp = -\lambda x$ . Let us now introduce the Legendre transform of  $h$  by  $h^* = h - p(dh/dp) = h - p\eta$ . From  $dh^* = -pd\eta$ , it follows that  $h^* = h^*(\eta) = h^*(-\lambda x)$ . Now, if we go back to eq.(2.19), we see that from  $h = -\lambda\zeta = -\lambda(px - y)$ , the ECS is expressed as  $y = (h + \lambda px)/\lambda = (h - p\eta)/\lambda$ . So, this shows that the ECS is connected directly with the free energy via  $y(x) = h^*(-\lambda x)/\lambda$ , which is Andreev's relation in 2-d.

In this way, by studying the equilibrium shapes of crystal we have the possibility to directly observe a free energy surface.

The fact that Andreev's relation holds is not at all accidental, since the Wulff construction is in reality a construction of a family of tangent planes (lines) to which the ECS is the envelope. As discussed in [49], it is this idea of tangency that is central to the Legendre transform. Namely, that a given curve (surface)  $y = y(x)$  ( $y = y(x_1, x_2)$ ) can be also represented as the envelope of a family of tangent lines (planes). So, any equation that gives us the family of tangent lines determines the curve equally well as the explicit relation  $y = y(x)$ . Since a straight line in 2-d may be described by two numbers  $p$  and  $b$ , where  $p$  is the slope and  $b$  is the intercept with the  $y$ -axis, a knowledge of the intercept  $b$  of the tangent lines as a function of the slope  $p$  enables us to construct

the family of tangent lines and also their envelope, which is just what the Wulff construction does. The way one computes the relation  $b = b(p)$  once  $y = y(x)$  is given is known as the Legendre transform [49]. So, from the point of view of the Wulff construction, Andreev's relation is a natural one.

There exists a magnetic analogy to Andreev's relation [45,49,50], first pointed out by Garcia et. al [51]. Namely, the one between the Gibbs  $G(T,H)$  and Helmholtz  $F(T,M)$  free energy for a simple ferromagnet at temperature  $T$  below the Curie temperature  $T_c$  ( $T < T_c$ ), where  $H$  is the magnetic field and  $M$  is the magnetization, given by  $M = -(\partial G/\partial H)_T$ . For magnetic systems the following relation holds [50]  $G(T,H) = F(T,M) - MH$ . Fig. 6. shows the relation between  $G(T,H)$  and  $F(T,M)$  for a fixed temperature  $T$  below  $T_c$ . The drawing of the figure utilizes the fact that  $G$  is a concave function of the magnetic field  $H$  and  $F$  is a convex and even function of the magnetization  $M$  [50].

The important point is the existence of a cusp in  $G(H)$  for  $H = 0$ , where the magnetization  $M(H)$  jumps from  $M(H=0^-) = -M_0$  to  $M(H=0^+) = M_0$  as the magnetic field changes sign. Following [49], a tangent to the curve  $G(H)$  at point  $(H,G(H))$  intercepts the  $H = 0$  axis at a height  $F$ , so that  $(F - G)/H = -(\partial G/\partial H) = M$  and we obtain that  $F = G + HM$ , which is the Legendre transformation between  $F$  and  $G$ . The point to note is that the cusp of  $G(H)$  at  $H = 0$  leads to a region of magnetizations between  $[-M_0, M_0]$  for which  $F(M)$  is not defined.

Now, the parallel between the Legendre transform of  $G$  and  $F$  and the Wulff construction of §2.4.1. (Fig. 3.) is obvious, where we can identify the ECS  $y(x)$  with the Gibbs free energy  $G$  and  $h(p)/\lambda$  with  $F(M)$ .

Pursuing the above analogy further, we can infer that whenever the ECS has corners, certain tangent planes (orientations) are missing (as already mentioned in §2.4.2.) and the surface tension  $\gamma$  is not defined for those directions.

So, the main conclusion of this analogy is [45] that when the ECS contains no corners, all tangent planes to the crystal shape are present and  $\gamma(\phi)$  is defined for all orientations. When the ECS is fully faceted, the surface tension  $\gamma(\phi)$  is not defined for certain orientations.

It should be pointed out that the ECS  $R(\theta)$  is defined for all values of  $\theta$ . Moreover, it is *continuous* and *convex* (for  $g = 0$ ). So. the orientation variable  $\theta$  is like a field variable (H), while  $\phi$  is the conjugate density variable (M) [14,45].

## 2.5. Chemical Potential of the Equilibrium Crystal Phase - the Effect of Curvature [18,19]

On the basis of a thermodynamic argument it is obvious that the value of the chemical potential  $\mu$  must be the same at all points of the ES at which it can be uniquely defined. Otherwise, the free energy could be lowered by redistribution of material.

Following Mullins [19], let us consider once again the familiar by now 2-d example, where the ECS is given by minimizing the energy functional eq.(2.17). If there is an infinitesimal rearrangement of material that gives a new surface  $y(x) + \delta y(x)$ , the corresponding change in the free energy will be (for constant T, V and  $\mu$ ) [19]

$$\delta F = \int (dh/dp) \delta p dx = \int (dh/dp) [d(\delta y)/dx] dx = - \int [d(dh/dp)/dx] \delta y dx \quad (2.29)$$

where  $\delta p = d(\delta y)/dx$  was used.

If the assumption is made that the chemical potential is defined at all points on the crystal surface, the same change in free energy is given by

$$\delta F = \mu \delta N = (\mu/v) \int \delta y dx \quad (2.30)$$

where  $v$  is the atomic volume and  $\delta y dx/v$  gives the number of atoms added to the interface due to the change in shape  $\delta y$  in the interval  $dx$ .

From eqs.(2.29) and (2.30) we arrive at (since  $\delta y$  is arbitrary)  $\mu = -vd(dh/dp)$  and after some algebraic manipulation we finally obtain

$$\mu = -v(\gamma + d^2\gamma/d\phi^2)(d^2y/dx^2)(1 + (dy/dx)^2)^{-3/2} = v(\gamma + d^2\gamma/d\phi^2)K \quad (2.31)$$

where  $\phi = \tan^{-1} p$  and  $K$  is the curvature of the surface and it is a function of position. Eq.(2.31) is a 2-d analogue of Herring's formula for the excess of the chemical potential at any point on a curved surface over that on a flat surface [18,19]

$$\mu = v[(\gamma + d^2\gamma/d\phi_1^2)K_1 + (\gamma + d^2\gamma/d\phi_2^2)K_2] \quad (2.32)$$

where  $K_1$  and  $K_2$  are the curvatures of the crystal surface in the planes of its principal sections and  $\phi_1$  and  $\phi_2$  are the angles of the tangent in these planes.

It should be noted that Herring's equation does not give the value of the chemical potential at orientations corresponding to cusps in the  $\gamma$ -plot, since at the cusps the second derivatives of  $\gamma$  with respect to the angles are infinite.

As it was pointed out in §2.3., for orientations, corresponding to close-packed crystal planes, the derivatives  $d\gamma/d\phi$  are discontinuous. Therefore, for low-index faces the supplementary chemical potential will be finite only when the curvatures  $K_1$  and  $K_2$  vanish and the corresponding surfaces become planes (in 2-d straight lines). This is the physical reason for the appearance of faces on the ECS.

At this point it is possible to determine the meaning of  $\lambda$ , the Lagrange multiplier of the variational problem that arises from the constant volume constraint. If we recall the Euler-Lagrange equation (2.18) for the variational problem (2.17), it is easy to show that  $d(\partial h/\partial p)/dx$  is equal to  $-(\gamma + d^2\gamma/d\phi^2)K = -\lambda$ . Comparing this with eq.(2.31) we see that  $v\lambda$  is the excess chemical potential, associated with a curved surface and it follows that  $\lambda$  has the dimensions of pressure. Since the excess chemical potential associated with an ECS (which is convex in the absence of gravity) is always positive it follows that  $\lambda$  is always positive for the gravity-free case.

## 2.6. Corner Points on Crystal Surfaces [52,53]

Since we have already mentioned in §2.4.2. and §2.4.5 that the ECS may contain corner points it is worth mentioning the thermodynamic conditions that are necessary to be fulfilled for the existence of corners (or



edges in 3-d). For the parts of the crystal that are bounded by a smooth shape, the chemical potential is determined by Herring's formula.

The conditions to be satisfied at the corner point of an ECS can be most easily derived from the solution of the variational problem (2.17) of a smooth curve with a self-intersecting point. By integrating eq.(2.18) we get that  $h(p) = -\lambda x + C$  (const.). Also noting that eq.(2.17) has a first integral  $h(p) + \lambda y - p[dh(p)/dp] = C_1$  (an integration constant), we get that  $\lambda y = p[dh(p)/dp] - h(p) + C_1$ . From the expressions for  $\lambda x$  and  $\lambda y$  we can derive the conditions to be satisfied at the corner, using the fact that the corner on the ECS  $(x_c, y_c)$  is a self-intersecting point. Namely,

$$h(p - p_+) = h(p - p_-)$$

$$(h(p) - p[dh(p)/dp])(x_c+0, y_c+0, p_+) = (h(p) - p[dh(p)/dp])(x_c-0, y_c-0, p_-)$$

where  $p_- = p_-(x_c-0)$  is the slope to the right and  $p_+ = p_+(x_c+0)$  is the slope to the left of the corner point  $(x_c, y_c)$  (recall that we are using a "left-handed" coordinate system).

As a final remark to this Chapter we should mention that the flat parts (facets) of the ES correspond to areas of zero curvature on the crystal surface, which means (for 2-d) that  $d^2y/dx^2$  vanishes (or equivalently  $d^2h^*/d\eta^2 = 0$ ). (In 3-d, where the ECS is described by a function  $z = z(x_1, x_2)$ , where the  $x_i$  ( $i = 1, 2$ ) are Cartesian coordinates, area of zero curvature means that both of the eigenvalues of the matrix  $\partial^2 z / \partial x_i \partial x_j$  ( $i, j = 1, 2$ ) become zero). When corners appear, they can be regarded (2-d) as jumps in  $dy/dx$  (or  $dh^*/d\eta$ ). From the above, the connec-

tion of the equilibrium crystal shapes with the general theory of phase transitions is obvious.

To summarize: equilibrium crystal shapes can develop facets, which are the result of the *anisotropy* of the surface tension of crystals. The upper bound for the dimension of the facet is proportional to the jump in the angle derivative of the surface tension at the corresponding orientation, which in turn is proportional to the step energy on that particular face. If the surface tension  $\gamma$  is known as a function of orientation, the equilibrium crystal shape is determined by the Wulff construction. The effect of a flat homogeneous substrate on the ECS is described by a generalized Wulff construction. The ECS and the function  $h(p)$  are related by a Legendre transformation (Andreev's relation), which has a magnetic analogy. The connection of the ECS with the theory of phase transitions is exhibited.

## CHAPTER 3

### EQUILIBRIUM SHAPE OF A CRYSTAL ADSORBED TO A WALL

As in the Introduction, the first in depth study of the effects of gravity on the equilibrium crystal shapes was the work of Avron et al. [21], where the sessile crystal was considered.

Here we consider a different form of support - pinning to a wall (vertical flat substrate). Physically, such "pinnings" frequently occur as a result of impurities. This particular choice of support (or boundary condition) was motivated by the experiment itself [1-4], where the hcp  $^4\text{He}$  crystals were grown from isolated nucleation sites on the walls of the container (see also [54]). To keep the problem simple and tractable (solvable), we consider only two dimensions with pinning at the top or bottom end of the crystal (the hung crystal). For 3-d crystals the case considered here is applicable to crystals with axial symmetry, held in suitable geometries.

A related problem, the equilibrium shape of a free or pinned meniscus (i.e. the equilibrium shape of the interface between a semi-infinite crystal or droplet and an ambient phase bounded by a vertical plane wall on one side) is also solved. The importance of this problem arises from the fact that the meniscus experiments are used to directly measure the surface tension between superfluid  $^4\text{He}$  and hcp  $^4\text{He}$  crystals, as well as the angle of contact between the interface and the container surface [1-4]. In order to determine the correct values of the surface tension and the contact angle from the experimental results, a solution of the

equilibrium shape of the meniscus between the superfluid and crystal phases for the geometry of the experimental cell is needed. Note also that the expression for the meniscus shape used to determine the surface tension and the angle of contact in [1-4] was that for an *isotropic* meniscus in a gravitational field. This expression describes the unfaceted part of the meniscus away from the container wall, and since in most cases the meniscus was faceted, the solution for the meniscus shape that we present here for the case of a *general (anisotropic)* surface tension may be of use in interpreting the available experimental data.

### 3.1. Crystal Pinned at Top

#### 3.1.1. The Variational Problem

To describe a crystal pinned to a wall in the presence of gravity, we need additional terms in the (free) energy functional, eq.(2.17), that correspond to the pinning and gravity. Referring to Fig. 7., the gravity term is simply  $-\rho g \int y x dy$ , the volume (area) is equal to  $V = \int x dy$ , where  $\rho$  is the difference between the densities of the crystal and the medium,  $\rho = \rho_c - \rho_m$ . Physically, the pinning may arise from the interaction of the crystal phase with impurities on an otherwise homogeneous wall. Mathematically, the pinning will impose a boundary condition on the solution of the Euler-Lagrange equation of the variational problem at hand. If we consider a single impurity localized at  $y = 0$ , i.e., the crystal is pinned to one point only, then we have to add a term  $J\delta(y)$  to  $\gamma_\Delta$  in the (free) energy functional, where  $J$  is the strength of the interaction. So,

in order to obtain the equilibrium shape of a crystal,  $x = x(y)$ , pinned to a wall in the presence of gravity we have to find the stationary point of the following energy functional ( $\theta(x) = 1(0)$  for  $x \geq 0$  ( $x < 0$ ))

$$F[x] - \lambda V = \int \theta(x) \{ [\gamma(q)(1+q^2)^{1/2} + \gamma_{\Delta} + J\delta(y)] - \lambda x - \rho g y x \} dy \quad (3.1)$$

The sign in the volume constraint term is clearly arbitrary, though it is chosen to conform to the  $g = 0$  limit, where  $\lambda > 0$ .

Fig. 7. shows the coordinate system used. The point the crystal is pinned on the wall is taken as the origin of the coordinate system. The position of the wall (substrate) is given by  $x = 0$ . The angles  $\omega_p$  and  $\omega_f$  are the angles the tangent to the equilibrium crystal shape makes at the support (pinning) point and at the free end with the positive  $y$ -axis. The gravitational force is directed along the positive  $y$ -axis.

Before presenting the solution, we should make the following remarks. First, because of gravity, the free energy functional  $F$  is strictly unbounded from below, even if it is constrained to fixed volume  $V$ . It can always be lowered by breaking the crystal into two pieces, one bit over the pin and another piece running off to  $y = \infty$ . So, the minimum we seek is a local one, corresponding to a connected crystal. Next we comment on the two "edges" of the crystal. At the free end,  $x = 0$  and the contact angle is (as it will be shown below)  $\omega_f$ , while  $y$  is an unknown. At the pinned end  $x = y = 0$ , while the contact angle  $\omega_p$  is an unknown. These unknowns ( $y, \omega_p$ ) will be functions of  $\lambda$  and  $g$ , which must be solved in terms  $V$  and  $g$ . Physically, we should expect that fixing  $V$  and increasing  $g$  (or vice versa) would increase the length of the crystal and decrease the

contact angle at the pinned end.

### 3.1.2. Equilibrium Shape of a Crystal Pinned at Top

The solution to the variational problem (eq. (3.1)) is given by the Euler-Lagrange equation (recall that the surface tension  $\gamma$  is an arbitrary function of  $\omega$ , which in turn depends on  $q = dx/dy$  via  $q = \tan\omega$ ), which consists of two parts. The first part comes from the terms that are proportional to  $\theta(x)$  and describe the region  $x > 0$ . It has the form

$$-\lambda - \rho gy = d(\gamma(q)q(1+q^2)^{1/2} + [d\gamma(q)/dq](1+q^2)^{1/2})/dy \quad (3.2)$$

which can also be written as (using eq. (2.22d))

$$\lambda + \rho gy = -d(\gamma(\omega)\sin(\omega) + [d\gamma(\omega)/d\omega]\cos(\omega))/dy = d[y_w(\omega)]/dy \quad (3.3)$$

The second part arises from the terms in the Euler-Lagrange equation that are proportional to  $\delta(x) = d\theta(x)/dx$ , namely,  $[\gamma_\Delta + J\delta(y) - \lambda x - \rho gyx + x_w(\omega)]$ . The bracketed expression, when equated to zero in order to satisfy the Euler-Lagrange equation, essentially gives the condition the ECS must satisfy for  $x = 0$ . So, for  $x(y=0) = 0$  (i.e., the free end of the crystal) we obtain that

$$x_w(\omega_f) = -\gamma_\Delta \quad (3.4)$$

We observe that the value of the angle  $\omega_f$  is the same as that obtained in

the gravity-free ( $g=0$ ) Wulff-Winterbottom construction (§2.4.4) using the the same substrate (see eq.(2.28c)). The physical intuition for this is that free contact angles depend on *local* conditions only and consequently should not depend on  $g$ . We also notice that at the pinned end of the crystal ( $y = x(y=0) = 0$ ), the condition the equilibrium shape must satisfy cannot be determined from the Euler-Lagrange equation, since the presence of the pinning term  $J\delta(y)$  in the energy functional does not allow the coefficient of  $\delta(x)$  (i.e., the bracketed expression above) to vanish. So, the angle  $\omega_p$  is an unknown. Thus, the Euler-Lagrange equation of the variational problem (3.1) leads to a non-linear differential equation and a boundary condition for the free end of the crystal.

Equation (3.3) can be integrated to give

$$y_w(\omega) = -[\gamma(\omega)\sin(\omega) + (d\gamma/d\omega)\cos(\omega)] - \lambda y + \rho g y^2/2 + C \quad (3.5)$$

At the point of pinning  $y = 0$ , the angle  $\omega$  equals  $\omega_p$  and the constant  $C$  is equal to  $-(\gamma(\omega_p)\sin(\omega_p) + [d\gamma/d\omega](\omega_p)\cos(\omega_p))$ , i.e.,  $C = y_w(\omega_p)$ . Note that the angle  $\omega_p$  is not determined yet. From eq.(3.5) it is trivial to solve for  $y(\omega)$  in terms of the Wulff shape

$$- \lambda/\rho g \pm [(\lambda/\rho g)^2 - 2K(\omega_p, \omega)/\rho g]^{1/2} \quad (3.6)$$

where  $K(\omega_p, \omega) = y_w(\omega_p) - y_w(\omega)$ .

From eq.(3.6) it follows that a choice of solution should be made for the physical shape  $y(\omega)$  based on which solution satisfies the boundary condition  $y(\omega_p) = 0$  at the pinned end. Thus, the choice of solution

depends on the value (sign) of  $\lambda$ .

As it has already been discussed, in this problem we also have the following boundary conditions for the x-coordinate of the ES

$$x(\omega_p) - x(\omega_f) = 0 \quad (3.7)$$

where the value of the angle  $\omega_f$  is determined from the generalized Young-Dupre equation  $x_w(\omega_f) = -\gamma_\Delta$  and the angle  $\omega_p$  is an unknown. Since  $dx = \tan(\omega)dy$ , then the x-coordinate is obtained in parametric form from the expression

$$x(\omega) = \int_{\omega_p}^{\omega} \tan(\omega) [dy/d\omega] d\omega \quad (3.8)$$

and we have used the condition  $x(\omega_p) = 0$ . The angle  $\omega_p$  is determined from the other boundary condition  $x(\omega_f) = 0$ .

Now, eqs.(3.6) and (3.8) give the required equilibrium crystal shape in parametric form and we can see that  $\lambda$ , the Lagrange multiplier that comes into the problem because of the constant volume constraint, enters as a parameter.

Since the value of  $\lambda$  is crucial for the choice of the solution that will describe the physical shape, it is important to see if the presence of gravity can force  $\lambda$  to attain also negative values in contrast to the gravity-free case, when  $\lambda$  is always positive (see §2.5.).

From thermodynamic considerations, by looking at the Gibbs free energy in the presence of an external potential  $U$ , one can arrive at the following condition for equilibrium (see [17], p. 74)



$$\mu_0(T,P) + U = \lambda = \text{const.} \quad (3.9)$$

where  $\mu_0(T,P)$  is the chemical potential in the absence of the external field,  $T$  is the temperature and  $P$  is the pressure. It is obvious that in the absence of an external potential  $\lambda$  is positive. From eq.(3.9) it follows that in the gravity case ( $g \neq 0$ ,  $U = -\rho gy$ )  $\lambda$  must absorb what appears to be an arbitrary constant coming from  $U$ . Therefore, it is not determined in sign. Consequently, in the presence of an external field, the choice of the solution as given by eqs.(3.6) and (3.8), namely, the choice of sign in front of the square root in eq.(3.6), is affected by the value of the external field, since  $\lambda$  can be positive, negative or zero. Now, if we perform the differentiation in eq.(3.2) we obtain

$$\lambda + \rho gy = - (\gamma + d^2\gamma/dw^2)(d^2x/dy^2)(1 + (dx/dy)^2)^{-3/2} \quad (3.10)$$

where  $-(d^2x/dy^2)/(1 + (dx/dy)^2)^{3/2}$  is the curvature at a given point on the equilibrium crystal shape. From eq.(3.10) we can see that  $\lambda$  is equal to the excess pressure within the crystal at the point of support, which we chose to be  $y = 0$ , with respect to a flat surface [18,19,22]. So, depending on the sign of  $\lambda$ , the equilibrium crystal shape may be convex or concave at the pinning point, i.e.,  $\lambda$  determines the curvature at  $y = 0$ .

From eq.(3.9) it follows (see also eq.(3.1)) that the combination  $\lambda + \rho gy$  plays the role of an *inhomogeneous* effective pressure (potential), i.e.,  $P_{\text{eff}} = \lambda + \rho gy$ . So, we see that when  $\lambda > 0$ , the crystal may exist in a region where the effective pressure is positive, i.e.  $P_{\text{eff}} > 0$ . How-

ever, if  $\lambda$  is negative, then there exists a  $y^*$  ( $= -\lambda/\rho g > 0$ ), such that the effective pressure is *negative* from  $y = 0$  to  $y^*$ . In this region the crystal is *concave*. On the other hand, the free (bottom) end of the crystal should be *always convex*, lying in a region where the effective pressure is positive. This is intuitively clear. So, in the  $\lambda < 0$  case there are necessarily two parts of the connected crystal which have effective pressure of different sign.

In what follows we will examine the parametric solution of the ECS for the two cases, corresponding to  $\lambda > 0$  and  $\lambda < 0$ .

When  $\lambda$  is positive ( $\lambda > 0$ ,  $P_{\text{eff}} > 0$ ), the solution of the equilibrium shape is given by

$$y(\omega) = -(\lambda/\rho g) + [(\lambda/\rho g)^2 - 2K(\omega_p, \omega)/\rho g]^{1/2} \quad (3.11)$$

where the (+) sign is chosen in front of the square root in eq.(3.6), in order to satisfy the boundary condition  $y(\omega_p) = 0$ .

For the x-coordinate of the ES we use eq.(3.8) and get

$$x(\omega) = -(1/\rho g) \int_{\omega_p}^{\omega} (\gamma + d^2\gamma/d\omega^2) \sin(\omega) [(\lambda/\rho g)^2 - 2K(\omega_p, \omega)/\rho g]^{-1/2} d\omega \quad (3.12)$$

The angle  $\omega$  varies in the interval  $[\omega_p \geq \omega \geq \omega_f]$  for both eqs.(3.11) and (3.12) and the resulting shape will be convex.

When  $\lambda$  is negative ( $\lambda < 0$ ), the solution of the ECS consists of two parts, corresponding to the regions of negative and positive effective pressure  $P_{\text{eff}}$ . For the region with negative effective potential we get

$$y(\omega) = (-\lambda/\rho g) - [(\lambda/\rho g)^2 - 2K(\omega_p, \omega)/\rho g]^{1/2} \quad (3.13)$$

where the condition  $y(\omega_p) = 0$  leads to the choice of the (-) sign in front of the square root in eq.(3.6).

The expression for the x-coordinate takes the form

$$x(\omega) - x'(\omega) = (1/\rho g) \int_{\omega_p}^{\omega} (\gamma + d^2\gamma/d\omega^2) \sin(\omega) [(\lambda/\rho g)^2 - 2K(\omega_p, \omega)/\rho g]^{-1/2} d\omega \quad (3.14)$$

In eqs.(3.13) and (3.14) the angle  $\omega$  changes in the range  $[\omega_p \leq \omega \leq \omega^*]$  (see §3.1.3 below) and the resulting equilibrium shape is concave. The angle  $\omega^*$  is determined from the condition

$$2K(\omega_p, \omega^*) = \lambda^2/\rho g \quad (3.15)$$

with  $y(\omega^*) = y^*$ . Note that the maximum magnitude  $\lambda$  can obtain ( $\lambda < 0$ ) is given by  $[2\rho g K(\omega_p, \omega_{\max}^*)]^{1/2}$ , where  $\omega_{\max}^*$  is the maximum value  $\omega^*$  can attain. Note also that the angle  $\omega^*$  should be such as to ensure the positivity of  $K(\omega_p, \omega^*)$ . The condition  $K(\omega_p, \omega^*) > 0$  also determines the direction in which the angle  $\omega$  must change, relative to  $\omega_p$ .

For the region with positive effective pressure (the y-coordinate taking values in the range  $y^* - y(\omega_f) \leq y \leq y(\omega_f)$ ) we chose the (+) sign in front of the square root in eq.(3.6) and the crystal shape is given by

$$y(\omega) = -(\lambda/\rho g) + [(\lambda/\rho g)^2 - 2K(\omega_p, \omega)/\rho g]^{1/2} \quad (3.16)$$

and

$$x(\omega) - x'(\omega^*) - (1/\rho g) \int_{\omega_p}^{\omega} (\gamma + d^2\gamma/d\omega^2) \sin(\omega) [(\lambda/\rho g)^2 - 2K(\omega_p, \omega)/\rho g]^{-1/2} d\omega \quad (3.17)$$

with  $\omega$  in the range  $\omega^* \geq \omega \geq \omega_f$ .

### 3.1.3. Results

To obtain the parametric expression for the equilibrium crystal shape we have used part of the boundary conditions, i.e.,  $x(\omega_p) = 0$  and  $y(\omega_p) = 0$ . The other boundary condition  $x(\omega_f) = 0$  leads to an equation for the contact angle  $\omega_p$  (see eqs.(3.12), (3.14) and (3.17)). This is not a simple equation for finding  $\omega_p$  as a function of  $\lambda$  and  $g$ . If we wish to find  $\omega_p$  in terms of the experimentally controllable parameters  $V$  and  $g$ , there is additional difficulty involved in finding the functional form of  $\lambda(V, g)$ . The equation  $x_w(\omega_f) = 0$  (that determines  $\omega_p(\lambda, g)$ ), together with the condition for the constant volume constraint give two equations for the determination of the two unknowns  $\omega_p$  and  $\lambda$ . Note also that when  $g \rightarrow 0$ , then the contact angle at the pinned end  $\omega_p(\lambda, g)$  goes into  $\omega_0$ , the corresponding angle of the (gravity-free) Wulff-Winterbottom construction with the same substrate (see Fig. 8.).

Thus, it is very surprising that for both cases of  $\lambda > 0$  and  $\lambda < 0$ , the volume of the crystal is given by

$$\rho g V = \int_{\omega_f}^{\omega_p} y [dx/d\omega] d\omega = x_w(\omega_p) - x_w(\omega_f) = x_w(\omega_p) + \gamma_{\Delta} \quad (3.18)$$

where both  $x_w$  and  $\gamma_\Delta$  are known gravity-free quantities. In deriving the above equation (3.18) we have used the (boundary) condition  $x(\omega_f) = 0$  and eq.(3.4). Note that  $\lambda$  does not appear explicitly in the above expression. An easy way to see why this is so (apart from performing the integration in eq.(3.18) with the explicit expressions for  $y$  and  $dx$ ) is to note that  $dx/dy = dx_w/dy_w$ . Thus, eq.(3.3) can be written as  $\lambda + \rho gy = d[x_w(\omega)]/dx$  and it is easily seen that the reason  $\lambda$  does not appear in the expression for the volume  $\rho gV = \rho g \int y dx$  is the vanishing of  $x$  at the top and bottom end of the crystal (see eq.(3.6)).

Eq.(3.18) is a very important result which gives the connection between the (total) volume of the crystal  $V$ , the gravitational acceleration  $g$  and the contact angle  $\omega_p$ . This equation provides an easy graphic determination of  $\omega_p$ , just as the Winterbottom construction determines  $\omega_o$ . Just plot the value of  $\rho gV$  on the x-axis of the Wulff-Winterbottom diagram and find the angle  $\omega$  it corresponds to. The angle  $\omega$  found in this way will be the desired angle  $\omega_p$ . Now, the boundary condition  $x(\omega_p) = 0$  (eq.(3.7)) gives an implicit equation to determine  $\lambda$  as a function of  $V$  and  $g$ . Once  $\omega_p$  and  $\lambda$  are found, all quantities on the right hand side of eqs.(3.6) and (3.8) are explicitly known.

One immediate consequence of eq.(3.18) is that there is a maximum value of  $\rho gV$  allowed, i.e.  $x_w(0) + \gamma_\Delta = \gamma(0) + \gamma_\Delta$ . For fixed  $g$ , this corresponds to a critical volume  $V_c$

$$V_c = [x_w(0) + \gamma_\Delta]/\rho g \quad (3.19)$$

beyond which there is no local minimum for the (free) energy functional,

even when the crystal is constrained to have a fixed volume. We may label this situation by the grandiose name: *gravitational induced wetting*. Physically, the (connected) crystal shape consists of an interface with infinitesimal thickness (zero volume) and arbitrary length  $L$ , starting at the pinning point and having finite surface in contact with the wall and the crystal attached at the bottom of the interface. The existence of the interface increases the surface energy by  $L[\gamma(0) + \gamma_{\Delta}]$ , while the crystal gains gravitational energy  $LgV$ . What eq.(3.19) says is that the energy cost of creating the wetting interface is exactly balanced by the gain in gravitational energy of the bulk crystal.

As the critical volume  $V_c$  is approached (i.e.,  $\omega_p \rightarrow 0$ ), we get from  $\rho g(V_c - V) = x_w(0) - x_w(\omega_p)$  (assuming that the Wulff shape is smooth and using eq.(2.22c)) that  $\omega_p$  goes to zero as  $(V_c - V)^{1/2}$ .

From eq.(3.18) we can also see that the value of the angle  $\omega_p$  cannot be greater than the corresponding angle  $\omega_0$  of the Wulff-Winterbottom construction, because the volume of the crystal must be positive (see also Fig. 8.), i.e.  $\omega_p < \omega_0$ .

From the same equation it follows that the crystal pinned at the top displays another interesting feature. As the volume of the crystal is increased ( $g$  being fixed), the corresponding angle  $\omega_p$  reaches the value  $\zeta$  for a certain value  $V^*$ , so that (see eq. (3.12))

$$\int_{\omega_f}^{\zeta} (\gamma + d^2\gamma/d\omega^2) \sin(\omega) [-2K(\zeta, \omega)/\rho g]^{-1/2} d\omega = 0 \quad (3.20)$$

where  $\lambda(V^*) = 0$  and  $K(\zeta, \omega) < 0$  in the range  $[\omega_f, \zeta]$ . When the volume  $V^*$  is exceeded, i.e.,  $V > V^*$ ,  $\lambda$  becomes negative. It should be mentioned that

$V^*$  is not so easy to determine as  $V_c$ ; one must first find the angle  $\zeta$  from eq.(3.20) and then determine  $V^*$  from  $V^* = [x_w(\zeta) + \gamma_\Delta]/\rho g$ .

Finally, relation (3.18) is verifiable experimentally by monitoring the changes in  $\omega_p$  as the crystal grows by using, for example, the same experimental technique as in [2,3].

Now let us see the implications the solutions of the equilibrium shape (for both  $\lambda > 0$  and  $\lambda < 0$ ) have for the morphology of the crystal.

When  $\lambda$  is positive ( $\lambda > 0$ ), or the volume of the crystal  $V$  is smaller than  $V^*$  ( $V < V^*$ ), the equilibrium crystal shape will be convex for the whole range of change of the angle  $\omega$ , [ $\omega_p \geq \omega \geq \omega_f$ ]. Since  $\omega_p < \omega_o$  (in order for the crystal volume to be positive), in the presence of gravity some crystallographic directions will be *missing* from the equilibrium crystal shape which otherwise will be present in the gravity-free case using the same substrate, namely, those between the angles  $\omega_o$  and  $\omega_p$ .

When  $\lambda$  is negative ( $\lambda < 0$  or  $V > V^*$ ), the equilibrium shape will always exhibit a *concave* part (eqs.(3.13) and (3.14)) in the region with negative effective pressure, where the angle  $\omega$  is in the range [ $\omega^* \geq \omega \geq \omega_p$ ]. Consider the two cases of partial wetting ( $\gamma_\Delta < 0$  and  $\gamma_\Delta > 0$ ) separately. For  $-\gamma(0) < \gamma_\Delta < 0$  ( $\omega_o < \pi/2$ ), it is easy to see, by looking at the Wulff- Winterbottom diagram (Fig. 8.), that in order for the condition  $K(\omega_p, \omega^*) > 0$  to hold,  $\omega$  must increase relative to  $\omega_p$ . For  $\gamma(\pi) > \gamma_\Delta > 0$  (when  $\omega_o > \pi/2$ ), the existence of a concave part in the equilibrium shape is only possible if  $\omega_p < \pi/2$  (so that eq.(3.10) is satisfied and the curvature of the crystal at the point of pinning is negative). By referring once again to Fig. 8., we see that in order for  $K(\omega_p, \omega^*) > 0$ ,  $\omega^* > \omega_p$  and  $\omega$  should increase relative to  $\omega_p$ . From Fig. 8.

it is clear that  $\omega_{\max}^* = \pi/2$ .

When  $\omega$  reaches  $\omega^*$ , the effective pressure becomes positive, and the crystal will have a convex shape in the range  $[\omega^* \geq \omega \geq \omega_f]$ . So, when  $\lambda$  is negative, the ECS will always contain both concave and convex parts.

In order to determine how the presence of gravity affects the orientations of the ES in this case ( $\lambda < 0$ ) we have to determine the values  $\omega^*$  can take. Consider  $V(\omega^*)$ , defined as the volume of the crystal that is enclosed by the ES between the points  $[x(\omega_f), y(\omega_f)]$  and  $[x(\omega^*), y(\omega^*) - y^*]$ , i.e., between the free end of the crystal and the point of  $P_{\text{eff}} = 0$ .

Since

$$\rho g V(\omega^*) = \int_{\omega_f}^{\omega^*} y [dx/d\omega] d\omega - \rho g x(\omega^*) y^* = x_w(\omega^*) - x_w(\omega_f) + \lambda x(\omega^*) - \rho g x(\omega^*) y^*$$

and  $\lambda = \rho g y^*$ , we see that  $V(\omega^*) = x_{wb}(\omega^*)/\rho g$ . Since the enclosed volume is positive, we have that  $x_{wb}(\omega^*) > 0 = x_{wb}(\omega_0)$  and hence  $\omega^* < \omega_0$ . So, in the  $\lambda < 0$  ECS, orientations between  $\omega_0$  and  $\omega^*$  will be *missing* compared to the gravity-free case with the same substrate.

Also from eq.(3.17), we deduce another feature of the ES of the crystal when it has both a concave and a convex part. The concave portion from  $y = 0$  to  $y = y^*$  is identical to the convex part from  $y = y^*$  to  $y = 2y^*$  rotated by  $180^\circ$  ( $y^* = -\lambda/\rho g$  is a point of inflection on the crystal shape).

To complete the discussion of the parametric solution of the equilibrium crystal shape, we study how the facet length is modified in the presence of gravity. For the two-dimensional crystal, the length of the facet, corresponding to a certain orientation  $\omega$ , is given by  $l = l(\omega) =$



$(y_- - y_+)/\cos(\omega)$ , where  $y_+$  is the value of the y-coordinate corresponding to the value of the derivative  $d\gamma/d\omega$  when the angle  $\omega$  is increasing and  $y_-$  corresponds to the value of  $d\gamma/d\omega$  when  $\omega$  decreases. From eq.(3.2), which we can put in the form  $y_w(\omega) = \lambda y + \rho g y^2/2 + C$ , we obtain

$$\ell_w(\omega) = \ell(\omega)(\lambda + \rho g y_c) = \ell(\omega)\rho g(y_c - y^*) = \Delta[d\gamma/d\omega] = 2\beta/a \quad (3.21)$$

where  $\ell_w(\omega) = \Delta[d\gamma/d\omega]$  is the length of the facet of the Wulff shape (see eq.(2.23) and recall that it is equal to the jump  $\Delta$  of the first derivative of the surface tension with respect to the angle  $\omega$ , which in turn gives the step free energy per unit length  $2\beta/a$  associated with a given facet [41]) and  $y_c = (y_- + y_+)/2$  is the center of the facet in question. Thus, from eq.(3.21) we offer a very convenient way to measure step free energies  $\beta$ , when the crystal displays an inflection point (i.e. when  $\lambda$  is negative or the crystal is sufficiently big,  $V > V^*$ ). Note that for the gravity-free case, since the equilibrium shape is scale invariant, the length of a facet is proportional to, but does not determine the step free energy  $\beta$ . However, in the presence of gravity, there exists an absolute length scale (the capillary length) and eq.(3.21) can be used to directly measure step free energies, since in this case the center of the facet  $y_c$  and the inflection point  $y^*$  (where the crystal changes its curvature) can be readily determined experimentally (note that in the  $\lambda < 0$  case,  $y^*$  is physical, i.e., it lies on the equilibrium shape itself).

### 3.2. Crystal Pinned at Bottom

Here we will consider the equilibrium shape of a crystal pinned to a wall at its lower end. This case is mathematically identical to that depicted in Fig. 7., but with the direction of the gravitational field reversed - Fig. 9. Physically, this situation appears if there is a large region (from the pinning point down) of the substrate that is coated with an impurity that repels the crystal. Note, that an effective reversal of the gravitational field occurs when the density of the finite volume phase is less than the density of the ambient phase (e.g., a bubble inside an infinite crystal). This new configuration will bring a change in sign in the potential energy term of the free energy functional (eq.(3.1)), so it is  $\rho gy$ . Note also, that the point of pinning is once again chosen as the origin of the coordinate system and that the end of the crystal  $y(\omega_f)$  is positive ( $y(\omega_f) > 0$ ). The corresponding Euler-Lagrange equation is

$$-\lambda + \rho gy = d\{\gamma(\omega)\sin(\omega) + [d\gamma(\omega)/d\omega]\cos(\omega)\}/dy = -d[y_w(\omega)]/dy \quad (3.22)$$

with the boundary condition  $x_w(\omega_f) = -\gamma_\Delta$  (the same as eq.(3.4)). Clearly, the boundary conditions for the x-coordinate, eq.(3.7) remain unchanged.

From the analogue of eq.(3.10) we see that  $\lambda$  has the usual meaning of excess pressure within the crystal at the point of support (at the bottom end) with respect to a flat surface and it determines the curvature at the pinning point, while the combination  $\lambda - \rho gy$  plays the role of an effective pressure  $P_{\text{eff}}$ . Since the curvature at the bottom end of the crystal (the support point in Fig. 9.) must be positive,  $\lambda$  is *always*

positive here. Otherwise, (i.e., if  $\lambda$  is negative) the crystal can never exist since its both ends will lie in a region where  $P_{\text{eff}} < 0$  (recall that the crystal extends towards the positive y-axis). Proceeding as before, eq.(3.22) can be integrated and from the resulting equation we get

$$y(\omega) = \lambda/\rho g - [(\lambda/\rho g)^2 - 2K(\omega, \omega_p)/\rho g]^{1/2} \quad (3.23)$$

where  $\omega_p$  is the angle at  $y = 0$ ,  $K(\omega, \omega_p) = y_\omega(\omega) - y_\omega(\omega_p)$  and the (-) sign is chosen in front of the square root because of the condition  $y(\omega_p) = 0$ .

The x-coordinate of the equilibrium shape is obtained from eq.(3.8) and it reads

$$x(\omega) = -(1/\rho g) \int_{\omega_p}^{\omega} (\gamma + d^2\gamma/d\omega^2) \sin(\omega) [(\lambda/\rho g)^2 - 2K(\omega, \omega_p)/\rho g]^{-1/2} d\omega \quad (3.24)$$

The angle  $\omega$  varies in the interval  $[\omega_p, \omega_f]$ .

The volume of the crystal  $V$  is given by

$$V = -[x_\omega(\omega_p) + \gamma_\Delta]/\rho g \quad (3.25)$$

and we can see that the value of the angle  $\omega_p$  must be greater than the corresponding angle  $\omega_o$  of the Wulff-Winterbottom construction,  $\omega_p > \omega_o$ , so as to ensure the positivity of the crystal volume. So, it follows that when the crystal is supported from the bottom end, new orientations, absent from the gravity-free one, will be present in the equilibrium crystal shape. The new orientations are in the range  $[\omega_p \geq \omega \geq \omega_o]$ . From eq. (3.25) it is also seen that the maximum value  $\rho g V$  can attain is given

by  $-\left[x_w(\pi) + \gamma_\Delta\right]$ .

In principle, the possibility exists that part of the crystal may lie in a region where the effective pressure is negative. To show that the equilibrium crystal shape in this case cannot exhibit a concave portion, we ask: does an angle  $\omega^*$  exist, so that  $y(\omega^*) = \lambda/\rho g$  (or  $2K(\omega^*, \omega_p) = \lambda^2/\rho g$ ) belongs to the equilibrium shape. Suppose that  $\omega^*$  existed, it is easily observed from the Wulff-Winterbottom construction that when the angle  $\omega$  becomes smaller than  $\omega^*$ , then  $2K(\omega, \omega_p) > \lambda^2/\rho g$  (since  $y_w$  increases as  $\omega$  decreases). But that means  $[(\lambda/\rho g)^2 - 2K(\omega, \omega_p)]^{1/2}$  will be imaginary. So, in this case no part of the equilibrium shape can be in a region with negative effective pressure and the shape is *always convex*.

### 3.3. Equilibrium Shape of a Free and Pinned Meniscus

Laplace formula, eq.(2.14), is used as the theoretical basis for the experimental measurement of the surface tension  $\gamma$  of a fluid-fluid interface via the capillary rise or depression method [34,55], where the pressure difference is given by the hydrostatic pressure inside the capillary. The surface tension is determined from the relation  $\gamma = \rho gLR/2$ , where  $L$  is the height of the interface in the capillary with respect to the position of the interface outside the capillary and  $R$  is the radius of curvature of the meniscus inside the capillary (the meniscus shape inside the capillary is assumed spherical). Even the first direct measurements of the surface tension between the solid and superfluid  $^4\text{He}$  were done by the capillary depression method [1] (the hcp  $^4\text{He}$  did not wet the copper surfaces used in the experiment), where the solid  $^4\text{He}$  was thought

as if it were an *isotropic fluid* rather than a crystal.

In the case of fluids, when the capillary radius is not small and the equilibrium meniscus is not spherical, in order to determine  $\gamma$  from the experimentally observed meniscus, the Laplace formula (eq.(2.14)) should be written as a differential equation for the equilibrium shape, using the differential expressions for the curvature radii. Even for the isotropic case, a general solution of this equation has not been obtained.

For the case of a crystal-fluid interface, when the meniscus may be faceted, the Laplace formula, because of the anisotropy of the surface tension, must be replaced by Herring's equation, eq.(2.32), for the un-faceted part of the meniscus. The determination of the surface tension of a crystal-fluid interface and the contact angle from the experimental observations require the solution of Herring's equation for the geometry of the set-up. To solve this 3-d problem analytically is quite hopeless. On the other hand, we can solve it in 2-d. Since the experimentally available data is a photograph of a 2-d section of the meniscus, the surface tension could then be found in principle by fitting the measured profile of the meniscus with the solution of Herring's equation in two dimensions. The contact angle could be found by comparing the experimental and calculated height of the meniscus.

Another approach to the meniscus problem, which we will follow, is to determine the equilibrium shape of the interface by minimizing the free energy. So, the problem at hand is to determine the ES of the interface of a semi-infinite crystal or fluid, bounded by a vertical plane wall on one side (at  $x = 0$ ) - Fig. 10. The interface extends into the  $x > 0$  region. Since we have an interface between two phases that corres-

pond to  $P_{\text{eff}} \neq 0$ , the interface will be located at  $P_{\text{eff}} = 0$ . One should also note the difference with the gravity-free case, where the semi-infinite (not closed) interface can only exist for  $\lambda = 0$ , which follows from Herring's equation. Recall from §2.5. that  $v\lambda$  is the excess chemical potential, associated with a curved surface and it vanishes for a plane interface. The contact point of the meniscus with the vertical wall will be taken as the origin of the coordinate system (Fig. 10.).

In order to determine the ES of the interface we have to minimize the free energy of the system, eq.(3.1). The general solution of the variational problem is still given by eq.(3.5)

$$y_w(\omega) = \lambda y + \rho g y^2 / 2 + C$$

but, with different boundary conditions, the solution here will be different.

For the case of a *free (unpinned)* meniscus, the boundary conditions are:

$$y(\omega_0) = 0 \text{ and } y(\pi/2) = y_0 = -\lambda/\rho g \quad (3.26)$$

The first comes from the contact angle for a free meniscus and is the usual  $\omega_0$  (where  $x_w(\omega_0) = -\gamma_\Delta$ ). The second states that the interface is horizontal ( $\omega = \pi/2$ ) far away from the wall, where  $y$  must reach a value to insure  $P_{\text{eff}} = 0$ .

Thus, If the crystal partially wets the substrate (wall) with  $\gamma_\Delta < 0$ , then  $\omega_0 < \pi/2$  and since  $\omega$  has to increase to  $\pi/2$  in order to satisfy the

boundary condition that at  $y = y_0$ ,  $\omega = \pi/2$ , the solution for this case (which will call wetting) is given by

$$y^{\text{wet}}(\omega) = y_0 - [2K(\omega, \pi/2)/\rho g]^{1/2} \quad (3.27)$$

where  $K(\omega, \pi/2) > 0$  (see Fig. 8. and note that at  $y_{\text{wb}} = 0$ ,  $\omega = \omega_0 < \pi/2$ ).

From eq.(3.27) we can see that at the contact point with the wall, where  $\omega = \omega_0$ ,  $y^{\text{wet}}(\omega_0) = 0 < y_0$  and the meniscus rises at the wall with respect to the interface far away from the wall (note that in our case the  $y$ -coordinate increases vertically downwards - Fig. 10.). The rise of the meniscus  $y_0$  is given explicitly by  $y_0 = [2K(\omega_0, \pi/2)/\rho g]^{1/2}$ . Since  $y_0$  is positive, it follows that  $\lambda < 0$  and the meniscus rises into the region where  $P_{\text{eff}} < 0$ . The same conclusion can be drawn if we compare eq.(3.27) with eq.(3.13) and note that both have the minus sign in front of the square root. This shows that both equations describe the ES in the region with  $P_{\text{eff}} < 0$ .

If  $\gamma_{\Delta} > 0$  (this case will be called non-wetting),  $\omega_0 > \pi/2$  and  $\omega$  has to decrease to the value of  $\pi/2$  in order to satisfy the boundary condition that  $y = y_0$  when  $\omega = \pi/2$ . The solution in this case is given by

$$y^{\text{non-wet}}(\omega) = y_0 + [2K(\omega, \pi/2)/\rho g]^{1/2} \quad (3.28)$$

where  $\omega_0 \geq \omega \geq \pi/2$  and  $K(\omega, \pi/2) > 0$ .

We can see that when  $\omega = \omega_0$ ,  $y^{\text{non-wet}}(\omega_0) = 0$  and  $y_0 < 0$ , so that the meniscus falls at the wall. If we compare eq.(3.28) with eq.(3.11) we note that both equations describe the region with  $P_{\text{eff}} > 0$ .

A question that follows naturally is what is the shape of two free menisci, separated by a vertical plane wall with both sides the same - Fig. 11. The position of the wall is given by  $x = 0$ . The contact point of the semi-infinite meniscus that extends into the  $x > 0$  region with the vertical wall is denoted by  $O$  and the contact angle between the meniscus and the wall is denoted by  $\omega_0$ . The contact point of the semi-infinite meniscus, that lies in the  $x < 0$  region, with the wall is denoted by  $O_1$  and the respective contact angle is  $\omega_0'$ . In what follows we will consider the wetting case ( $\gamma_\Delta < 0$ ) only.

The solution for the shape of the meniscus in the  $x > 0$  region is exactly the one for the single semi-infinite meniscus bounded by a vertical wall and is given by eq.(3.27). The contact angle  $\omega_0$  is determined from the relation  $x_w(\omega_0) = -\gamma_\Delta$  (eq.(3.4)).

The profile of the semi-infinite meniscus that lies in the  $x < 0$  region is described again by the general solution, eq.(3.5), with different contact angle  $\omega_0'$ , that has to be determined.

We can determine  $\omega_0'$  in two ways. First, we can use the analytic result, presented in §3.1.2., modified to describe the  $x < 0$  region ( $x$  goes into  $-x$ ) and we can directly arrive at the relation  $x_w(\omega_0') = \gamma_\Delta$ , that will determine the contact angle  $\omega_0'$ . Note the absence of the minus sign when compared to eq.(3.4). The other way to obtain the contact angle  $\omega_0'$  is to use the Wulff-Winterbottom construction. We note that the fixed orientation of the wall  $m$ , with respect to the wetting interface, which lies in the  $x > 0$  region, is  $m = -x$ , where  $x$  is the unit vector in the positive  $x$ -direction. The contact angle, obtained from eq.(3.4), is the angle  $\omega_0$  of the Wulff-Winterbottom diagram in Fig. 8. The fixed orienta-



tion of the wall  $m'$ , with respect to the wetting meniscus of the  $x < 0$  region is  $m' = x$ . If we now plot  $\gamma_{\Delta}x$  on the Wulff-Winterbottom diagram in Fig. 8., we obtain the diagram shown in Fig. 12. We see that this corresponds exactly to the angle  $\omega_0'$  being determined from the relation  $x_w(\omega_0') = \gamma_{\Delta}$  ( $\gamma_{\Delta} < 0$ ). We also note that the angle  $\omega_0' > \pi/2$ .

To summarize, both wetting menisci in the  $x < 0$  and in the  $x > 0$  region exhibit new orientations  $\omega$  that are not present on the gravity-free ECS adsorbed on the same wall. If we look at Fig. 12., the new orientations correspond to the angles the tangents at all points of the portion PAP' of the Wulff-Winterbottom shape make with the positive y-axis. The points P and P' on the Wulff shape have tangents, which make angles  $\omega_0$  and  $\omega_0'$  respectively, with the positive y-axis. For the meniscus in the  $x > 0$  region, these new orientations are in the range  $\omega_0 < \omega \leq \pi/2$  and for the meniscus in the  $x < 0$  region they are in the range  $\omega_0' \geq \omega \geq \pi/2$ .

The equilibrium profile of the meniscus in the  $x < 0$  region is thus described by eq.(3.27) with  $\omega_0' \geq \omega \geq \pi/2$  and  $K(\omega, \pi/2)$  always positive. Note that the value of the rise of the 'left' meniscus at the wall is  $y(\omega_0') = y_0 - [2K(\omega_0', \pi/2)/\rho g]^{1/2}$  and it is different from the rise of the 'right' meniscus, which is  $y_0 = [2K(\omega_0, \pi/2)/\rho g]^{1/2}$ . Thus, we see that in general, the two menisci will have a different rise at the wall and there will be a discontinuity of the solution of the meniscus profile at the wall. The value of this discontinuity is given by

$$[2K(\omega_0, \pi/2)/\rho g]^{1/2} - [2K(\omega_0', \pi/2)/\rho g]^{1/2}$$

and it shows that the reason for the discontinuity of the solution of the

meniscus profile at the wall is the *asymmetry* of the  $\gamma$ -plot around  $\pi/2$ . Had the  $\gamma$ -plot been symmetric around  $\pi/2$  (as it is in cubic crystals), the difference in the rise of the two menisci would have been zero and the solution of the meniscus profile would have been continuous at the wall.

As a final remark to the case of the free meniscus we point out that for the isotropic ( $\gamma = \text{const.}$ ) case, eqs.(3.27) and (3.28) take the form

$$y(\omega) = y_0 \mp [(1 - \sin\omega)2\gamma/\rho g]^{1/2} = y_0 \mp a(1 - \sin\omega)^{1/2} \quad (3.29)$$

where the (-)/(+) sign corresponds to the wetting/non-wetting case,  $a$  is the capillary length and  $\mp(1 - \sin\omega_0)^{1/2}$  gives the capillary rise/depression of the meniscus at the wall. Eq.(3.29) reproduces the result obtained in [40] by using the Laplace formula.

Note that the equilibrium shape of the free meniscus is invariant under translations in  $y$ . So, by choosing the contact point to be  $y = 0$ ,  $y_0$  (and  $\lambda$ ) is obtained through  $[2K(\omega_0, \pi/2)\rho g]^{1/2}$ . If we *pin* the meniscus to the wall, then,  $y_0$  is fixed by external controls (as the level of the pin above the asymptotic interface). Now, the pinning angle,  $\omega_p$ , is an unknown and will be given in terms of  $y_0$ . We consider this case next.

When the meniscus is pinned to the wall (at  $x = 0$ ,  $y = 0$ ), the boundary condition is that at the point of pinning  $y = 0$ ,  $\omega = \omega_p$  and the solution is given by

$$y(\omega) = y_0 \pm [y_0^2 - 2K(\omega_p, \omega)/\rho g]^{1/2} \quad (3.30)$$

where (+)/(-) corresponds to the pinning of the meniscus below ( $P_{\text{eff}} > 0$ ) or above ( $P_{\text{eff}} < 0$ ) relative to the semi-infinite interface.

From the condition that  $y = y_0$  when  $\omega = \pi/2$ , we obtain the following relation that must be satisfied by  $\omega_p$

$$K(\omega_p, \pi/2) - y_w(\omega_p) - y_w(\pi/2) = \rho g y_0^2 / 2$$

or

$$y_w(\omega_p) = y_w(\pi/2) + \rho g y_0^2 / 2 \quad (3.31)$$

This is the equation giving  $\omega_p$  explicitly as a function of  $y_0$ .

When the distance  $y_0$  is increased (experimentally this can be achieved by varying the size of the observation cell), the pinning angle  $\omega_p$  will change until it reaches the value 0, when the pinning is above the interface or the value  $\pi$ , when the pinning is below the interface. For pinning above the interface, when  $y_0$  exceeds the value  $(2[y_w(0) - y_w(\pi/2)]/\rho g)^{1/2}$ , wetting of the wall will be induced for a distance  $d$  from the pinning point given by (see also eq.(3.27))

$$d = y_0 - [2K(\omega_0, \pi/2)/\rho g]^{1/2}$$

For pinning below the interface, when  $(2[y_w(\pi) - y_w(\pi/2)]/\rho g)^{1/2}$  is less than the magnitude of  $y_0$  (here  $y_0$  is negative), the induced wetting of the wall will have a length  $d$  ( $d$  being positive, see also eq.(3.28))

$$d = -y_0 - [2K(\omega_0, \pi/2)/\rho g]^{1/2}$$

The excess volume  $\Delta V$ , corresponding to the wetting meniscus (i.e., free or pinned meniscus above the interface) is given by (see Fig. 10.)

$$\Delta V = \int x dy - x_o y_o - \int_{\omega_i}^{\pi/2} y [dx/d\omega] d\omega = [x_w(\omega_p) - x_w(\pi/2)] / \rho g \quad (3.32)$$

where  $i = p, o$  and

$$\rho g x(\pi/2) - \rho g x_o = \int_{\omega_i}^{\pi/2} (\gamma + d^2\gamma/d\omega^2) \sin(\omega) [y_o^2 - 2K(\omega_p, \omega) / \rho g]^{-1/2} \quad (3.32a)$$

is finite.

For the free meniscus, bounded by a wall, that extends into the  $x < 0$  region,  $\rho g x(\pi/2) - \rho g x_o'$  is negative and it is obtained from eq.(3.32a) when the lower limit of integration  $\omega_i$  is replaced by  $\omega_o'$ .

Eq.(3.32) also describes the depleted volume ( $\Delta V < 0$ ), corresponding to a free non-wetting or pinned meniscus below the interface with the appropriate algebraic value (note that for a non-wetting meniscus,  $\omega_p > \pi/2$  and  $x_w(\omega_p) < 0$ ).

Next we will consider the equilibrium shape of a free two-dimensional wetting meniscus between two parallel vertical flat walls - Fig. 13. The coordinate system  $(x', y')$  is chosen in such a way that the  $y'$  axis coincides with the left vertical wall. The point of contact of the meniscus between the vertical walls with the left wall is taken as the origin of the coordinate system. The separation between the walls is  $s$ .

It should be noted that the ES of the meniscus for both outside and between the walls is obtained by minimizing the (free) energy functional, eq.(3.1), and the solution of the meniscus profile is given everywhere by

eq.(3.5), with discontinuities at  $x' = 0$  and  $x' = s$ . As already pointed out, when the case of the two wetting menisci, separated by a vertical wall was considered, one of the reasons for these discontinuities is the asymmetry of the  $\gamma$ -plot around  $\omega = \pi/2$ . Another physical reason for the appearance of these discontinuities will be discussed below. The contact angles the free menisci make with the vertical walls,  $\omega_0$  and  $\omega_0'$ , are again given by the relations  $x_w(\omega_0) = -\gamma_\Delta$  and  $x_w(\omega_0') = \gamma_\Delta$ , for both outside and between the walls (we assume that both sides of the wall are the same). Note also that  $\omega_0$  is the contact angle when the menisci approach the walls from the right and  $\omega_0'$  is the contact angle when the menisci approach the walls from the left (see Figs. 11. and 13.).

For  $x'$ , that varies from  $-\infty$  to 0 and from  $s$  to  $\infty$ , the solution is that of a free semi-infinite meniscus described by eq.(3.26) with the boundary condition  $y(\pi/2) = y_0$  (i.e., when the angle  $\omega$  reaches  $\pi/2$ , the meniscus joins the interface far from the wall), which in the  $(x',y')$ -coordinate system becomes  $y'(\pi/2) = y(\pi/2) + \epsilon = y_0 + \epsilon$ , where  $\epsilon$  is the discontinuity of the solution at the opposite walls (see Fig. 13.).

Having obtained the solutions of the free (eq.(3.26)) and the pinned (eq.(3.30)) meniscus, it is not difficult to obtain the solution of the meniscus between the two parallel vertical walls. For  $x'$  between the vertical walls ( $x'$  in the range  $[0,s]$ ), the solution is given again by equation (3.26), but the value of the parameter  $\lambda$  is in general different from that in the semi-infinite case, which we shall denote by  $\lambda'$ . Recall that  $\lambda$  is the curvature of the meniscus at the point of contact with the vertical wall. If the separation of the two walls is larger than  $x_0 - x_0'$ , then the value of  $\lambda'$  is the same as that for the semi-infinite meniscus,

i.e., the shape of the meniscus between the walls is determined by each wall separately. If  $s < x_0 - x_0'$  (which is the experimentally interesting case), then the value of  $\lambda'$  is different from that for the semi-infinite meniscus and in this case it is determined from the condition  $x'(\omega_0') = s$ .

What we are interested in is to obtain an expression for the rise of the meniscus between the walls with respect to the location of the semi-infinite interface outside and far from the walls. Eq.(3.5) for the ES of the meniscus between the walls takes the form

$$y'(\omega) = -\lambda'/\rho g - [(\lambda'/\rho g)^2 - 2K(\omega_0, \omega)/\rho g]^{1/2} \quad (3.33)$$

where we have used that at the point of contact with the wall  $y' = 0$ , the angle  $\omega = \omega_0$ . Note also that since we are considering the wetting case, the (-) sign was chosen in front of the square root,  $K(\omega_0, \omega)$  is equal to  $y_w(\omega_0) - y_w(\omega)$  as usual and  $\omega_0 \leq \omega \leq \omega_0'$ , where  $\omega_0'$  is the angle of contact of the meniscus with the right wall, determined from  $x_w(\omega_0') = \gamma_\Delta$ .

The x-coordinate of the equilibrium meniscus profile is given by

$$x'(\omega) = \int_{\omega_0}^{\omega} (\gamma + d^2\gamma/d\omega^2) \sin(\omega) / \rho g [(\lambda'/\rho g)^2 - 2K(\omega_0, \omega)/\rho g]^{1/2} d\omega \quad (3.34)$$

The boundary condition  $x'(\omega_0') = s$ , which is used to determine  $\lambda'$ , is given by the following explicit expression

$$x'(\omega_0') = s = \int_{\omega_0}^{\omega_0'} (\gamma + d^2\gamma/d\omega^2) \sin(\omega) / \rho g [(\lambda'/\rho g)^2 - 2K(\omega_0, \omega)/\rho g]^{1/2} d\omega \quad (3.35)$$

From eqs.(3.33)-(3.35) follows that the ES of the meniscus between the two walls exhibits the same new orientations  $\omega$  as the two wetting semi-infinite menisci, separated by a vertical wall (see Fig. 12.), namely those in the range  $\omega_0 < \omega \leq \omega'_0$ , as compared to the wetting ECS on the same substrate.

The rise of the meniscus between the walls  $h$  is defined as the distance between  $y'(\pi/2) = d$  and the location of the semi-infinite interface away from and outside the wall, which is obtained from eq.(3.27) when  $\omega$  is equal to  $\pi/2$ , i.e.,  $h = y_0 + \epsilon - d$ . The problem is now to evaluate the discontinuity of the meniscus solution at the opposite walls  $\epsilon$ .

From the solution of the wetting semi-infinite meniscus, eq.(3.27), we obtain the relation  $y_0^2 = 2K(\omega_0, \pi/2)$  which enables us to write the expression for  $y'(\pi/2)$  in the form  $y'(\pi/2) = y_1 - [y_1^2 - y_0^2]^{1/2}$ , where  $y_1$  is equal to  $-(\lambda'/\rho g)$ . Since  $y_0$  and  $y_1$  are real positive numbers ( $y_0 \neq y_1$ ), we get that  $y_1 > y_0$  and  $\lambda' < \lambda$ . Recalling that the expression  $\lambda' + \rho g y'$  is the effective pressure at  $y'$  and that  $\lambda$  is the effective pressure of the semi-infinite meniscus at the wall, it is easy to see that the discontinuity of the solution at the opposite walls will be given by  $y' = \epsilon$ , so that  $\lambda' + \rho g \epsilon = \lambda$  or  $\epsilon = (\lambda - \lambda')/\rho g$ . Thus, for the rise of the meniscus between the walls,  $h$ , we finally obtain the expression

$$h = [(\lambda'/\rho g)^2 - 2K(\omega_0, \pi/2)/\rho g]^{1/2} \quad (3.36)$$

So, for a given wall separation  $s$  we can determine  $\lambda'$  from eq.(3.35) and then obtain the rise of the wetting meniscus between the walls (in the 2-d capillary),  $h$ , from eq.(3.36).

If the wall separation  $s$  tends to zero, from physical considerations we will expect that the curvature will tend to infinity (the shape of the wetting meniscus will be concave, so that  $\lambda'$ , which is negative, and it will tend to  $-\infty$ ). This can be also seen directly from eq.(3.35). So, in the case of a very small wall separation, eq.(3.35) becomes

$$s = \int_{\omega_0}^{\omega_0'} (\gamma + d^2\gamma/d\omega^2) \sin(\omega) d\omega / (-\lambda')$$

which after we solve for  $-\lambda'$  we obtain that  $-\lambda' = [x_w(\omega_0) - x_w(\omega_0')]/s$  and for  $h$  we get that  $h = -\lambda'/\rho g = [x_w(\omega_0) - x_w(\omega_0')]/\rho g s$ . For the isotropic case and small wall separation the meniscus rise is given by  $h = 2\gamma \cos(\omega_0)/\rho g s$ , which can be obtained directly from the Laplace equation when the meniscus shape is assumed to be circular [55].

It is worth noting that the solution of the ES of a crystal, pinned to a vertical wall in the presence of gravity (eqs.(3.11) to (3.17)) and the solution of the meniscus problem (eq.(3.30)), although looking alike, are entirely different solutions, arising from the same variational problem - the minimization of the total free energy of the system. Namely, eqs.(3.11) and (3.12) describe the whole ECS for  $\lambda > 0$ . Eqs.(3.13) and (3.14) describe the ECS in the  $P_{\text{eff}} < 0$  region (when  $\lambda < 0$ ) and they are patched at  $P_{\text{eff}} = 0$  with eqs.(3.16) and (3.17), that describe the ECS in the  $P_{\text{eff}} > 0$  region, to give the whole ES of the crystal for  $\lambda < 0$ . On the other hand, eq.(3.30) describes the ES of the meniscus up to  $P_{\text{eff}} = 0$  (i.e., up to the point  $(x_0, y_0)$ ), where it is patched by the solution of the semi-infinite interface, which is described by the equation  $dy/dx = 0$  and  $y(\pi/2) = y_0$ .



## CHAPTER 4

### EQUILIBRIUM SHAPE OF A PENDANT CRYSTAL

In this Chapter we will treat the equilibrium shape of a two-dimensional crystal hanging from a horizontal support, i.e., the ES of a pendant crystal. The ES of a pendant liquid drop has been extensively studied since the beginning of the century, primarily in connection with the measurement of the surface tension of liquids [56], the underlying physical intuition being that the ES of the pendant drop (the same is also valid for the pendant crystal) would be determined by the balance of the forces due to gravity, surface tension and the hydrostatic pressure.

Recently, the problem of the ES of pendant liquid drops and their stability has been considered by E. Pitts [22,57] and by D. H. Michael and co-workers [23,24], who also give extensive references to earlier work. The important contribution of the above papers and especially those by E. Pitts [12,57] was to point out that the maximum equilibrium volume attainable before the liquid droplet breaks is not so much determined by gravitational forces overpowering surface tension as the instability of the equilibrium shape to perturbations. The papers [12,23,24,57] are the first to discuss in detail the stability of the equilibrium pendant liquid drops.

In the following presentation we are not going to discuss the stability of the 2-d pendant crystal. Although we attempted to perform a stability analysis, the problem turned out to be very complicated and not tractable. When evaluating the maximum volume that a pendant crystal can

attain, we will use a physically intuitive condition for the onset of instability rather than a rigorously proven mathematical one.

In order to determine the ES of the pendant crystal we have to minimize, as usual, the total free energy of the system subject to the condition that the volume (area) of the crystal is constant. In this case, the equilibrium shape to be determined from the minimization of the (free) energy functional is most conveniently expressed as  $y = y(x)$  with  $dy/dx = \tan\phi = p$ . The geometry of the problem is shown in Fig. 14. The position of the horizontal support is given by  $y = 0$ . The origin of the coordinate system is chosen at the left contact point of the crystal with the substrate. The contact angles of the crystal with the support at the origin and at the right end with respect to the positive x-axis are denoted by  $\phi_0$  and  $\phi_1$  respectively.

The (free) energy functional, whose stationary point gives the ES of the pendant crystal, takes the form

$$F[y] - \lambda V = \int [\gamma(p)(1 + p^2)^{1/2} + \gamma_{\Delta} - \lambda y - \rho g y^2/2] \theta(y) dx \quad (4.1)$$

where the volume (area) of the crystal is given by  $V = \int y dx$  and  $-\rho g y^2 dx/2$  is the gravitational potential energy of a crystal strip with width  $dx$  and height  $y$ .

From eq.(4.1) we see that the integrand, which we will denote by  $\mathcal{L}$ , does not contain  $x$  explicitly, i.e.,  $\mathcal{L} = \mathcal{L}(y,p)$ . It is a well-known fact in the calculus of variations that in this case a first integral exists to the variational problem and it is given by  $\mathcal{L} - p(d\mathcal{L}/dp) = C$ , where  $C$  is a constant to be determined by the boundary conditions. Explicitly,

the first integral, which describes the region  $y > 0$ , is written as

$$\gamma(\phi)\cos(\phi) - (d\gamma/d\phi)\sin(\phi) + \gamma_{\Delta} - \lambda y - \rho g y^2/2 = C \quad (4.2)$$

where we have used  $dp = d\phi/\cos^2(\phi)$ .

If we use eq.(2.22b), eq.(4.2) takes the form

$$y_w(\phi) + \gamma_{\Delta} - \lambda y - \rho g y^2/2 = C \quad (4.3)$$

If we now continue the solution at the origin of the coordinate system, where at  $y = 0$ ,  $\phi = \phi_0$ , we obtain that the constant  $C = y_w(\phi_0) + \gamma_{\Delta}$ . Now we have to find the boundary conditions the ECS must satisfy for  $y = 0$ . These are given, exactly as in Chapter 3, by the terms in the Euler-Lagrange equation, corresponding to the energy functional, eq.(4.1), that are proportional to  $\delta(y) = d\theta(y)/dy$ . Namely, these terms are  $[y_w(\phi) + \gamma_{\Delta}]$ , which for the two ends of the crystal in contact with the horizontal support give the gravity-free contact angle equations (as expected)

$$y_w(\phi_0) = -\gamma_{\Delta} \quad \text{and} \quad y_w(\phi_1) = -\gamma_{\Delta} \quad (4.4)$$

which determine the angles  $\phi_0$  and  $\phi_1$ .

So, it follows that  $C = 0$  and from eq.(4.3) we can easily express  $y(\phi)$  in the form

$$y(\phi) = -\lambda/\rho g \pm [(\lambda/\rho g)^2 - 2K(\phi_0, \phi)/\rho g]^{1/2} \quad (4.5)$$

with  $K(\phi_0, \phi) = y_w(\phi_0) - y_w(\phi)$  as usual.

Note that the dependence of the equilibrium shape of the pendant crystal on the volume  $V$  will come only through  $\lambda$ , since the angles  $\phi_0$  and  $\phi_1$ , determined from eq.(4.4), do not depend on the crystal volume, as it is the case for the crystal pinned to a vertical wall, where  $w_p$  depends on the volume of the crystal.

Since  $dx = dy/\tan(\phi)$  and  $x(\phi_0) = 0$ , the x-coordinate of the ES of the pendant crystal is obtained in parametric form from

$$x(\phi) = \int_{\phi_0}^{\phi} dy/\tan(\phi) = I(\phi_0, \phi) \quad (4.6)$$

As in Chapter 3, a choice of solutions in eq.(4.5) should be made for the physical shape  $y(\phi)$ , based on which solution satisfies the boundary condition  $y(\phi_0) = 0$  or  $y(\phi_1) = 0$ . It is obvious that the choice will depend on the sign of  $\lambda$ . The explicit form of the Euler-Lagrange equation for the variational problem, eq.(4.1), is given by

$$\lambda + \rho gy = -[\gamma + d^2\gamma/d\phi^2](d^2y/dx^2)[1 + (dy/dx^2)]^{-3/2} \quad (4.7)$$

where we have used once again  $dp = d\phi/\cos^2(\phi)$ .

From eq.(4.7) we see that  $(\lambda + \rho gy)$  is the effective pressure  $P_{\text{eff}}$  at  $y$  and  $\lambda$  is the effective pressure at the plane of support.

It will be convenient for future use to express eq.(4.7) in the form

$$\lambda + \rho gy = d[x_w(\phi)]/dx \quad (4.8)$$

where we have used the expression for  $x_w(\phi)$  given by eq.(2.22a).

When  $\lambda > 0$ , the whole crystal is in a region with  $P_{\text{eff}} > 0$  and the solution for the y-coordinate of the equilibrium pendant crystal is

$$y(\phi) = -\lambda/\rho g + [(\lambda/\rho g)^2 - 2K(\phi_0, \phi)/\rho g]^{1/2} \quad (4.9)$$

From the condition that  $y \geq 0$  it also follows that  $K(\phi_0, \phi) < 0$  for all angles  $\phi$  in the range  $[\phi_0, \phi_1]$ , the function  $K$  being zero for  $\phi = \phi_0$  and  $\phi = \phi_1$ . From the Wulff-Winterbottom construction on Fig. 5. it follows that the angle  $\phi$  decreases, i.e.,  $\phi_0 \geq \phi \geq \phi_1$ , as the crystal is traversed from the origin to the right end.

When  $\lambda < 0$ , part of the crystal will be in a region with  $P_{\text{eff}} < 0$  and for this part of the crystal the y-coordinate of the physical shape is described by

$$y(\phi) = -\lambda/\rho g - [(\lambda/\rho g)^2 - 2K(\phi_0, \phi)/\rho g]^{1/2} \quad (4.10)$$

and since  $y \geq 0$ ,  $K(\phi_0, \phi) > 0$  for all  $\phi$ , except the contact angles and from Fig. 5. we see that the angle  $\phi$  should increase with respect to  $\phi_0$ , in order to ensure the positivity of  $K(\phi_0, \phi)$ .

Since the bottom part of the pendant crystal is always in a region where the effective pressure is positive (i.e., the bottom part is convex in order for the crystal shape to be closed), there exists a point  $y^*$  on the crystal where the ECS changes from concave to convex. At that point  $P_{\text{eff}} = 0$  and  $y^* = -\lambda/\rho g$  and the angle  $\phi$  reaches the value  $\phi^*$  ( $y(\phi^*) = y^*$ ), determined from the condition  $2K(\phi_0, \phi^*) = \lambda^2/\rho g$ .

The crystal shape in the region with  $P_{\text{eff}} > 0$  ( $y > y^*$ ) is given by choosing the (+) sign in eq.(4.5)

$$y(\phi) = -\lambda/\rho g + [(\lambda/\rho g)^2 - 2K(\phi_0, \phi)/\rho g]^{1/2} \quad (4.11)$$

Since  $y$  is real, the angle  $\phi$  should now decrease from  $\phi^*$ . If  $\phi$  were to further increase after reaching  $\phi^*$ , then  $2K(\phi_0, \phi)$  would exceed the value  $\lambda^2/\rho g$ , as seen from Fig. 5., and  $y$  would become imaginary. Now, as the  $\phi$  decreases, after passing through zero, it will reach a value  $\phi = \phi_1^*$ , such that  $2K(\phi_0, \phi_1^*) = \lambda^2/\rho g$ . In other words, as the parameter  $\phi$  varies, the  $y$ -coordinate reaches its maximum value at the bottom of the crystal, where  $\phi = 0$ , and continues on to the point  $y(\phi_1^*) = y^*$ . Thus, when  $\lambda < 0$ , the ES for the pendant crystal will have two inflection points.

When the  $y$ -coordinate re-enters the  $P_{\text{eff}} < 0$  ( $y < y^*$ ) region, the solution is given once again by eq.(4.10) and the angle  $\phi$  now varies in the range  $\phi_1^* \leq \phi \leq \phi_1$ . Note also that  $K(\phi_0, \phi_1) = 0$ .

There are explicit expressions for the  $x$ -coordinate of the physical shape, given by eq.(4.6), that correspond to eqs.(4.10) and (4.11) and differ only in the sign of  $dy$ , which is obtained from eq.(4.5)

$$dy = (\pm) -[\gamma(\phi) + d^2\gamma/d\phi^2]\cos(\phi)[(\lambda/\rho g)^2 - 2K(\phi_0, \phi)/\rho g]^{-1/2}d\phi/\rho g \quad (4.12)$$

where the (+) and (-) signs correspond to the  $P_{\text{eff}} > 0$  and  $P_{\text{eff}} < 0$  regions respectively.

If we denote by  $dy_1$  the choice of the (+) sign in eq.(4.12) and the corresponding integral in eq.(4.6) by  $I_1(\phi_0, \phi)$ , then the length of the

line of contact  $L$  between the crystal and the support will be given by  $L = x(\phi_1) - I_1(\phi_0, \phi_1)$  for the  $\lambda > 0$ . If we denote by  $dy_2$  the choice of the (-) sign in eq.(4.12) and the corresponding integral in eq.(4.12) by  $I_2(\phi_0, \phi)$ , then  $L$  for the  $\lambda < 0$  case will be given by  $L = I_2(\phi_0, \phi^*) + I_1(\phi^*, \phi_1^*) + I_1(\phi_1^*, \phi_1)$ . It is obvious that the dependence of  $L$  on the volume  $V$  comes solely through  $\lambda$ .

In order to obtain the volume of the equilibrium pendant crystal we note that eq.(4.8) can be written in the form  $ydx = (-\lambda dx + dx_w)/\rho g$ . So,

$$V = \int_{\phi_0}^{\phi_1} \frac{1}{y} [dx/d\phi] d\phi = (-\lambda/\rho g)L + [x_w(\phi_1) - x_w(\phi_0)]/\rho g \quad (4.13)$$

Eq.(4.13) is valid for both  $\lambda < 0$  and  $\lambda > 0$ . It gives the relationship between the crystal volume  $V$  and the parameter  $\lambda$ . Now, if we give a value to  $\lambda$ , this determines  $L$  and consequently  $V$ , for a fixed  $g$ . The appearance of the length of the line of contact between the support and the crystal, scaled by  $\lambda$ , in the expression for the volume, may reflect the existence of translational invariance in the plane of the support (the  $x$ -direction). From the above expression we also see that a critical volume  $V^*$  exists,

$$V^* = [x_w(\phi_1) - x_w(\phi_0)]/\rho g \quad (4.14)$$

and when it is reached, the curvature at the plane of support becomes zero ( $\lambda = 0$ ). Note that  $V^*$  is determined by the substrate-crystal interaction,  $\gamma_\Delta$ , which determines the contact angles  $\phi_0$  and  $\phi_1$  via eq.(4.4).

As it was already mentioned in the beginning of this Chapter, we do not have any rigorous criterion, as in the case of a crystal hung on a

vertical substrate, to determine the maximum volume attained by the pendant crystal before breaking. Instead, the condition for breaking that we will use is based on physical intuition. Namely, when the pendant crystal develops a neck, i.e.,  $\phi^*$  or  $\phi_1^* = \pi/2$  or  $-\pi/2$ , the ECS becomes unstable and if the volume is further increased, the crystal will eventually break. Of course, there exists a sufficient condition for the breaking of the crystal and that is when the crystal gets pinched.

According to our criterion, the non-wetting crystal ( $\gamma_\Delta > 0$ ) can never attain its maximum volume, because it becomes unstable when  $\lambda$  becomes negative. This follows directly from the discussion after eq.(4.10) since when  $\gamma_\Delta > 0$ ,  $\phi_0 > \pi/2$  and if the angle  $\phi$  has to increase with respect to  $\phi_0$ , it means that the non-wetting crystal develops a neck the moment the volume  $V^*$  is exceeded and the crystal will be unstable.

For the wetting case ( $\gamma_\Delta < 0$  and  $\phi_0 < \pi/2$ ), the condition for the onset of instability corresponds to a  $\lambda_c < 0$  and a volume  $V_c$  that exceeds  $V^*$ . In other words, the instability arises after the wetting crystal has developed a concave part. This critical volume  $V_c$  is given by

$$V_c = (-\lambda_c/\rho g)L_c + [x_w(\phi_1) - x_w(\phi_0)]/\rho g \quad (4.15)$$

where  $\lambda_c = -[2\rho gK(\phi_0, \pi/2)]^{1/2}$  and  $L_c$  is obtained from the corresponding expression given above by substituting the angles  $\phi^*$  or  $\phi_1^*$  with  $\pi/2$  and  $-\pi/2$  respectively. We also notice that the wetting crystal will not be able to attain its maximum volume, which is obtained for both the wetting and the non-wetting crystal, when  $\phi^* = \pi$  and  $\phi_1^* = -\pi$ .

The expression for the facet length  $l$  in the case of a pendant crys-



tal is obtained in exactly the same way as that for a crystal, supported by a vertical substrate (Chapter 3) and is also given by eq.(3.21).

Finally, we note that the ES of the pendant crystal will develop new orientations  $\phi$ , given by  $\phi_0 < \phi \leq \phi^*$  and  $\phi_1^* \leq \phi < \phi_1$ , for  $\lambda < 0$  when compared to the gravity-free case with the same substrate. If the stability criterion were correct, the new orientations will appear on wetting crystals only.

## CHAPTER 5

### EQUILIBRIUM SHAPE OF A CRYSTAL ON AN INCLINED SUBSTRATE

As discussed in the Introduction (see also [15,21]), in the presence of gravity, the way the crystal is supported affects the resulting equilibrium crystal shape. In Chapters 3 and 4 we discussed two types of support that were very particular in a certain way. For the hung crystal, translational invariance was broken along the direction of support. For the pendant crystal, translational invariance was preserved along the line of support. The physical reason for the breaking of translational invariance is that gravity introduces an inhomogeneous effective pressure (chemical potential)  $\lambda + \rho gy$  along the  $y$ -axis.

In the former case, the contact angle  $\omega_p$  and  $\lambda$  are the two unknowns to be determined in terms of the experimentally controllable parameters  $V$  and  $g$  in order to obtain the ECS (see §3.1.3). Fortunately, the equations used to determine  $\omega_p$  and  $\lambda$  were *not coupled* (see eqs.(3.18) and (3.7)).

In the case of a preserved translational invariance along the support,  $\lambda$  is the *only* unknown to be determined in terms of  $V$  and  $g$  (see eq. (4.13)) in the parametric solution of the equilibrium shape.

The interest in considering the equilibrium shape of a crystal on an inclined support stems from the fact that the plane (line) of support is along neither of the two specific directions mentioned above. So, in this case we would expect that the equations that determine the unknowns of the solution in terms of  $V$  and  $g$  to be more complicated.

In order for the crystal to be supported by an inclined plane, the

crystal should be pinned to the substrate, as it is the case of the hung crystal.

At first glance, it seems convenient to work in the (X,Y)-coordinate system (see Fig. 15.), where the position of the substrate is given by  $X = 0$ . What we notice though, is that the force of gravity has components along both coordinate axes X and Y. In this case, the translational invariance of the (free) energy functional is broken along both axes. If the equilibrium crystal shape is given by  $X = X(Y)$ , the energy functional  $F - \lambda V$  takes the form ( $dX/dY = Q$  and  $\theta$  is the angle between the inclined plane and the y-axis)

$$\int [\gamma(Q)(1 + Q^2)^{1/2} + \gamma_{\Delta} - \rho g \cos(\theta)XY + \rho g \sin(\theta)X^2/2 - \lambda X] \theta(X) dY$$

The corresponding Euler-Lagrange equation is very difficult to solve and the result cannot be easily interpreted in physical terms.

The moment we realize that the ECS on an inclined support may be considered as the equilibrium shape of a hung crystal sliced by the substrate at an angle  $\theta$ , then it is natural to work in the (x,y)-coordinate system (see Fig. 15.).

In what follows we will only consider the geometrical arrangement shown in Fig. 15., i.e., the crystal is supported by the inclined plane from below. The point the crystal is pinned to the support is taken as the origin of the coordinate system. The (x,y)-coordinate system is the same as that of Fig. 7., the gravitational field being directed along the positive y-axis. The inclined plane is at an angle  $\theta$  ( $0 \leq \theta \leq \pi/2$ ), measured counterclockwise from the positive y-axis. The second coordinate

system (X,Y) has also as its origin the point of pinning, but it is rotated around the origin with respect to the (x,y)-system, so that the Y-axis coincides with the substrate. The position of the inclined plane is given by  $X = 0$ , or equivalently by  $x\cos(\theta) - y\sin(\theta) = 0$ . The angles  $\omega_p$  and  $\omega_f$  have the usual meaning, i.e., they are the angles the tangent to the equilibrium crystal shape makes with the positive y-axis at the point of support and at the free end respectively, and  $\alpha$  is the angle the tangent to the ECS makes with the inclined plane (i.e., the positive Y-axis) with  $\alpha = \omega - \theta$ .

The ES of the crystal,  $x = x(y)$ , is obtained from the following (free) energy functional  $F[x] - \lambda V$  ( $q = dx/dy = \tan(\omega)$ )

$$\int [\gamma(q)(1 + q^2)^{1/2} + \gamma_{\Delta}/\cos(\theta) - \lambda x - \rho gyx] \theta [x\cos(\theta) - y\sin(\theta)] dy \quad (5.1)$$

where a total derivative of  $y$  has been omitted and the  $dy/\cos(\theta)$  factor of  $\gamma_{\Delta}$  takes into account the length of the interface between the crystal and the substrate.

The analysis of the ES of a crystal on an inclined plane proceeds in exactly the same way as that of the hung crystal in Chapter 3.

The Euler-Lagrange equation of the variational problem, eq.(5.1), that describes the region above the inclined substrate [ $x\cos(\theta) - y\sin(\theta) > 0$  or  $X > 0$ ] is

$$\lambda + \rho gy = d[y_{\omega}(\omega)]/dy \quad (5.2)$$

where we have used eq.(2.22c).

Eq.(5.2) can be also written in the form

$$\lambda + \rho gy = - (\gamma + d^2\gamma/d\omega^2)(d^2x/dy^2)(1 + (dx/dy)^2)^{-3/2} \quad (5.3)$$

which is, not surprisingly, exactly the same as eq.(3.10).

From eq.(5.3) we see once again that  $\lambda$  and  $\lambda + \rho gy$  have their usual meaning, namely,  $\lambda$  is the effective pressure at the point of support, which is chosen to be  $y = 0$ , and  $\lambda + \rho gy$  is the effective pressure  $P_{\text{eff}}$  at point  $y$ .

Eq.(5.2) can be trivially integrated and using the fact that at the pinned end  $y = x = 0$ , the angle  $\omega = \omega_p$  (where  $\omega_p$  is an unknown to be determined),  $y(\omega)$  of the physical shape is expressed as

$$y(\omega) = (-\lambda/\rho g) \pm [(\lambda/\rho g)^2 - 2K(\omega_p, \omega)/\rho g]^{1/2} \quad (5.4)$$

where  $K(\omega_p, \omega) = y_w(\omega_p) - y_w(\omega)$ .  $y(\omega)$  is explicitly specified when  $\lambda$  is given and  $\omega_p$  is determined.

It is also evident from the above equation that a choice of solution for the physical  $y(\omega)$  should be made for the different signs of  $\lambda$ . This choice is based on which solution satisfies the boundary condition  $y(\omega_p) = 0$  at the point of pinning. Note also that the angle  $\omega_p$  should be larger than  $\theta$  ( $\omega_p > \theta$ ), otherwise the crystal will wet the substrate ( $\alpha = \omega - \theta$ ). When  $\lambda > 0$ , the (+) sign is chosen and when  $\lambda < 0$ , the (-) sign is chosen in front of the square root.

At the free end of the crystal, the angle  $\omega_f$  is determined from the boundary condition that is given by the terms in the Euler-Lagrange equa-

tion that are proportional to  $\delta[x\cos(\theta) - y\sin(\theta)]$ . So. for the free end of the crystal we obtain the following contact angle equation

$$x_w(\omega_f)\cos(\theta) - y_w(\omega_f)\sin(\theta) = -\gamma_\Delta \quad (5.5)$$

and we immediately recognize that the left-hand side is nothing else but  $X_w(\alpha_f)$  and we have that  $(\alpha_f = \omega_f - \theta)$

$$X_w(\alpha_f) = -\gamma_\Delta \quad (5.6)$$

which is exactly the equation we would have expected.

Having determined  $\omega_f$ , then  $y(\omega_f)$  will determine  $L$ , since  $y(\omega_f) = L\cos(\theta)$ , where  $L$  is the length of the interface between the crystal and the support, with  $\omega_p$  still an unknown.

The  $x$ -coordinate of the ES is obtained in parametric form from the expression  $(dx = \tan(\omega)dy)$

$$x(\omega) = \int_{\omega_p}^{\omega} \tan(\omega)[dy/d\omega]d\omega \quad (5.7)$$

where the condition  $x(\omega_p) = 0$  is used.

Recall that in Chapter 3, although the length of the crystal-support interface was not known (i.e.,  $y(\omega_f)$  is an unknown), we were able to determine  $\omega_p$ , since  $x(\omega_f)$  had a definite value, namely, zero.

In the case of an inclined substrate, if the angle  $\omega_p$  were to be determined by the boundary condition  $x(\omega_f) = L\sin(\theta)$ , we see that it would not be possible, since  $L$  is an unknown too. So, we eliminate  $L$  by using

$$y(\omega_f)\tan(\theta) = x(\omega_f):$$

$$\{(-\lambda/\rho g) \pm [(\lambda/\rho g)^2 - 2K(\omega_p, \omega)/\rho g]^{1/2}\}\tan(\theta) = \int_{\omega_p}^{\omega_f} \tan(\omega) [dy/d\omega] d\omega \quad (5.8)$$

This is one equation for the two unknowns  $\lambda$  and  $\omega_p$ . The other equation comes from the volume constraint. Proceeding as in Chapter 3 and using  $V = \int xdy - [y(\omega_f)]^2 \tan(\theta)/2$ , we obtain

$$\rho g V = [x_{\omega}(\omega_p) - x_{\omega}(\omega_f)] + \lambda x(\omega_f) + x(\omega_f)y(\omega_f)/2 \quad (5.9)$$

where  $\omega_p \geq \theta$  and  $0 \leq \theta \leq \pi/2$ .

Now eqs.(5.8) and (5.9) give two equations for the determination of the two unknowns  $\lambda$  and  $\omega_p$  as functions of  $V$  and  $g$ , which look rather formidable. It is easily seen that there is no easy way of obtaining either  $\omega_p$ , as it is the case for the hung crystal, or  $\lambda$  in the case of the pendant crystal, as functions of the crystal volume  $V$ . This complication arises because of the general position of the substrate, so that the influence of both the preserved and broken translational invariance on the ECS is exhibited.

We note that when  $\theta$  is equals to zero, we recover the result for the hung crystal, given by eq.(3.18) and the boundary condition, eq.(3.4). When  $\theta = \pi/2$ , we recover the corresponding expressions for the sessile drop, given in [46].

Finally, we will show that for the sessile crystal  $\lambda$  can never become zero, i.e., the curvature at the support point of the sessile crystal is always positive. This follows directly from the expression for the

length  $L$  of the crystal-substrate interface. When  $\theta = \pi/2$ ,  $\omega_p$  becomes  $\omega_0$ , the corresponding angle of the Wulff-Winterbottom construction with the same substrate. Then, when  $\lambda > 0$ , eq.(5.7) reads

$$L = \int_{\omega_p}^{\omega_f} [dy_w(\omega)/d\omega] \tan(\omega) [(\lambda/\rho g)^2 - 2K(\omega_p, \omega)/\rho g]^{-1/2} d\omega/\rho g \quad (5.10)$$

and we see that since  $\omega_p > \theta = \pi/2$ ,  $\lambda$  cannot become zero, since if  $\lambda = 0$ , then as  $\omega$  goes from  $\omega_p$  to  $\pi/2$ , the value of  $-K(\omega_p, \omega)$  will be negative as seen from the corresponding Wulff-Winterbottom construction, Fig. 8., and the square root will become imaginary. The physical reason for this is that the sessile crystal will never have a closed shape if  $\lambda$  becomes negative, since then the top of the crystal, which should be convex with positive effective pressure, would end up being in a region with smaller effective pressure than the pressure at the support.



## CHAPTER 6

### SUMMARY AND OUTLOOK

The effects of gravity on the two-dimensional equilibrium shapes of crystals and menisci are investigated for different geometries (positions) of the substrate.

In the gravity-free case, the equilibrium crystal shape (ECS) is characterized by a *scale invariance*, i.e., the equilibrium shape (ES) the crystal attains is independent of its volume. As expected, based on physical considerations, the presence of gravity breaks the scale invariance and the resulting ECS changes as the volume of the crystal  $V$  is changed. Moreover, the presence of gravity breaks the translational invariance along the direction it acts. Physically realized by the necessity of a support, this is manifested by the existence of an *inhomogeneous effective pressure*  $P_{\text{eff}}$ , which divides the space into two regions, with  $P_{\text{eff}}$  either negative or positive. The ECS changes as the crystal passes from one region to another, being *concave* where  $P_{\text{eff}} < 0$ , and *convex* where  $P_{\text{eff}} > 0$ .

In all cases it was possible to express the corresponding ECS in terms of the gravity-free one.

For the hung crystal, i.e., a crystal pinned to a vertical wall at the top, it is shown that some orientations are *missing* from the ECS that otherwise will be present in the gravity-free ECS, adsorbed on the same substrate. Thus, facets could disappear from the crystal shape as the volume  $V$  or the gravitational acceleration  $g$  is increased. A critical volume  $V_c$  is found, so that if the crystal volume  $V$  exceeds  $V_c$ , the crystal

cannot be pinned. The ECS can exhibit both concave and convex portions.

For a crystal, pinned to a vertical wall at its lower end, we find that it will never develop a concave part. On the other hand, *new orientations*, absent from the gravity-free crystal, will be present on its ECS.

The ES of a free and pinned crystal meniscus is also solved and an expression for the excess (depleted) volume  $\Delta V$  is derived. The solution for the crystal meniscus between two walls is also presented.

For the pendant crystal, i.e., a crystal hanging from a horizontal support, we find that it can exhibit both concave and convex portions on its ECS. When it develops a concave part, *new orientations* will appear, compared to the gravity-free case. An intuitive stability criterion is introduced, according to which only crystals wetting the substrate can develop a concave portion before they break.

The treatment of a crystal on an inclined substrate shows the complications that arise in determining the ES for a general position of the support as a result of the conflict between the directions associated with gravity and support.

An expression for the facet length in the presence of gravity is obtained that is valid for all types of support. For crystal shapes that display a concave portion it offers a very convenient way to experimentally measure step free energies. Thus, by breaking scale invariance, the presence of gravity allows absolute measures of surface energy in contrast to the gravity-free case, where the facet length is proportional to the step free energy by an unknown scale.

In the following will touch upon some problems that are relevant to the present work.

The solution of the problem of the ECS in 3-d in the presence of gravity does not seem to be possible, at least for the present. As it is discussed in [46], the Euler-Lagrange equation of the variational problem of the ECS leads to a non-linear partial differential equation. Moreover, the breaking of scale and translational invariance in the presence of a field, does not allow for the existence of a construction similar to that of Wulff.

The ECS were obtained by finding the stationary point of the (free) energy functionals (3.1), (4.1) and (5.1), which satisfy the Weierstrass condition for a strong minimum. Namely, we studied the first variation of the (free) energy functional.

The problem of stability of the ECS is connected with the second variational problem that considers small deviations from the extremum. Only those ECS that are stable will be ultimately realized experimentally. The treatment of the fluctuations of the crystal shape is very difficult and not much theoretical work has been done [15].

In our treatment of the ECS in the presence of gravity, the orientation of the crystal relative to the substrate was fixed. If we allow the relative orientation to vary, then  $\gamma_{\Delta}$  will become a function of the orientation too,  $\gamma_{\Delta} = \gamma_{\Delta}(n)$ , and the resulting equilibrium crystal-substrate orientation should be found from the extremum of the (free) energy functional. The introduction of  $\gamma_{\Delta}(n)$  will complicate the problem immensely. We are not aware of any attempts to obtain the ECS when the orientation of the crystal-substrate interface is not fixed, even for gravity-free cases.

In our study of the ECS in the presence of gravity we made the

assumption that the external field does not affect the surface tension  $\gamma(n)$ . If this assumption is dropped, then the ECS will be influenced by both the external field and the changing  $\gamma$ . There is an experimental example that equilibrium liquid crystal shapes change when subject to an electric field [58,59]. The change of the ES is shown to be due to the change in  $\gamma(n)$  and so the crystal shape is obtained from a Wulff construction for the modified  $\gamma(n)$ . It would be interesting to find an experimental example where both the effect of the external field and the changing  $\gamma(n)$  are felt by the ECS.

At last we would like to point out the striking similarity that exists in the formal expressions for the determination of the critical value of  $\lambda = 0$  in the case of the ECS and the critical value  $\mu = 0$  in the case of Bose condensation [35,60]. Since  $\lambda$  is connected with the curvature of the ECS, which was shown to be connected with the second derivative of the Legendre transform of the free energy (§2.6) and Bose condensation is a first order phase transition (which does not exist in two-dimensions [60]), maybe this similarity points to a formal connection between a second order phase transition in the presence of an external field and a first order phase transition at a higher dimension and it may have some relevance to the theory of phase transitions in the presence of an external field, which is a very speculative statement.

## REFERENCES

1. S. Balibar, D. O. Edwards and C. Laroche, *Phys. Rev. Lett.* 42(1979) 782.
2. J. E. Avron, L. S. Balfour, C. G. Kuper, J. Landau, S. G. Lipson and L. S. Schulman, *Phys. Rev. Lett.* 45(1980)814.
3. J. Landau, S. G. Lipson, L. M. Määttänen, L. S. Balfour and D. O. Edwards, *Phys. Rev. Lett.* 45(1980)31.
4. K. O. Keshishev, A. Ya. Parshin and A. B. Babkin, *Zh. Eksp. Teor. Fiz.* 80(1980)716, Engl. tr. *Soviet Phys. JETP* 53(1981)362.
5. J. C. Heyraud and J. J. Métois, *J. Cryst. Growth* 50(1980)571.
6. J. C. Heyraud and J. J. Métois, *Acta Metall.* 28(1980)1789.
7. J. J. Métois, G. O. Spiller and J. A. Venables, *Phil. Mag.* A6(1982) 1015.
8. J. J. Métois and J. C. Heyraud, *J. Cryst. Growth* 57(1982)487.
9. J. C. Heyraud and J. J. Métois, *Surf. Sci.* 128(1983)344.
10. J. J. Métois and G. Le Lay, *Surf. Sci.* 133(1983)422.
11. C. Rottman and M. Wortis, *Phys. Rev.* B24(1982)6274.
12. J. E. Avron, H. van Beijeren, L. S. Schulman and R. K. P. Zia, *J. Phys.* A15(1982)L81.
13. C. Jayaprakash, W. F. Saam and S. Teitel, *Phys. Rev. Lett.* 50(1983) 2017.
14. C. Rottman and M. Wortis, *Phys. Rep.* 103(1984)59.
15. R. K. P. Zia, in *Statistical and Particle Physics - Common Problems and Techniques*, ed. K. C. Bowler and A. J. McKane (SUSSP Publications, Univ. of Edinburgh, 1984) pp. 247-301.
16. G. Wulff, *Z. Kristallogr. Mineral.* 34(1901)449.
17. C. Herring, *Phys. Rev.* 82(1951)87.
18. C. Herring, in *Structure and Properties of Solid Surfaces*, ed. R. Gomer and C. S. Smith (Univ. of Chicago Press, Chicago, 1953) pp. 5-72.
19. W. W. Mullins, in *Metal Surfaces: Structure, Energetics and Kinetics*, ed. W. D. Robertson and N. A. Gjostein (American Society for Metals,

Metals Park, Ohio, 1963) pp. 17-66.

20. W. L. Winterbottom, *Acta Metal.* 15(1967)303.
21. J. E. Avron, J. E. Taylor and R. K. P. Zia, *J. Stat. Phys.* 33(1985)49.
22. E. Pitts, *J. Fluid Mech.* 59(1973)753.
23. S. R. Majumdar and D. H. Michael, *Proc. R. Soc. London, Ser. A* 351(1976)89.
24. D. H. Michael and P. G. Williams, *Proc. R. Soc. London, Ser. A* 354(1977)117.
25. R. Finn, *Pacific J. Math.* 88(1980)549 and references therein.
26. N. Cabrera and N. Garcia, *Phys. Rev.* B25(1982)6057.
27. J. E. Taylor, *Asterisque* 118(1984)243.
28. L. A. Bol'shov, V. L. Pokrovski and G. V. Uimin, *J. Stat. Phys.* 38(1985)191.
29. J. E. Avron and R. K. P. Zia, to be published.
30. A. V. Babkin, D. B. Kopeliovitch and A. Ya. Parshin, *Zh. Eksp. Teor. Fiz.* 89(1985)2288, Engl. tr. *Soviet Phys. JETP* 62(1985)1322.
31. J. W. Gibbs, On the equilibrium of heterogeneous substances, reprinted in *Scientific Papers*, Vol.1 (Dover, New York, 1961).
32. J. W. Cahn, in *Interfacial Segregation*, ed. W. C. Johnson and J. M. Blakely (American Society for Metals, Metals Park, Ohio, 1979) pp. 3-23.
33. R. B. Griffiths, in *Phase Transitions in Surface Films*, ed. J. G. Dash and J. Ruvalds (Plenum Press, New York, 1980)pp. 1-27.
34. G. Navascués, *Rep. Prog. Phys.* 42(1979)1131.
35. L. D. Landau and E. M. Lifshitz, *Statistical Physics, Part 1*, 3-rd edition (Pergamon Press, Oxford, 1980).
36. A. F. Andreev and Yu. A. Kosevich, *Zh. Eksp. Teor. Fiz.* 81(1981)1435, Engl. tr. *Soviet Phys. JETP* 54(1981)761.
37. V. I. Marchenko and A. Ya. Parshin, *Zh. Eksp. Teor. Fiz.* 79(1980)257, Engl. tr. *Soviet Phys. JETP* 52(1980)129.
38. P. Nozières and D. E. Wolf, *Z. Phys. B-Condensed Matter* 70(1988)399.
39. D. E. Wolf and P. Nozières, *Z. Phys. B-Condensed Matter* 70(1988)507.

40. L. D. Landau and E. M. Lifshitz, *Fluid Mechanics* (Pergamon Press, Oxford, 1966).
41. L. D. Landau, in *Collected Papers of L. D. Landau*, ed. D. ter Haar (Oxford University Press, New York, 1965)p. 540.
42. W. K. Burton, N. Cabrera and F. C. Frank, *Phil. Trans. Roy. Soc. A243* (1951)299.
43. W. W. Mullins, *J. Math. Phys.* 3(1962)754.
44. A. F. Andreev, *Zh. Eksp. Teor. Fiz.* 80(1981)2042, Engl. tr. *Soviet Phys. JETP* 53(1982)1063.
45. M. Wortis, in *Fundamental Problems in Statistical Mechanics VI*, ed. E. G. D. Cohen (North-Holland, Amsterdam, 1985)p. 87.
46. R. K. P. Zia, to be published in *Proceedings of 1988 Workshop on Statistical Mechanics*, Academia Sinica, Taiwan, ed. C. K. Hu (World Scientific, Singapore, 1988).
47. R. K. P. Zia, J. E. Avron and J. E. Taylor, *J. Stat. Phys.* 50(1988) 727.
48. A. W. Adamson, *Physical Chemistry of Surfaces*, 3rd edition (John Wiley, New York, 1976).
49. H. B. Callan, *Thermodynamics* (John Wiley, New York, 1960)pp. 90-95.
50. H. E. Stanley, *Introduction to Phase Transitions and Critical Phenomena* (Clarendon Press, Oxford, 1971)ch. 2.
51. N. Garcia, J. J. Saenz and N. Cabrera, *Physica* 124B(1984)251.
52. I. M. Lifshitz and A. A. Chernov, *Kristallografiya* 4(1959)788, Engl. tr. *Soviet Phys. Crystallography* 4(1960)746.
53. A. A. Chernov, *Usp. Fiz. Nauk* 73(1961)277, Engl. tr. *Soviet Phys. Uspekhi* 4(1961)116.
54. S. Balibar, B. Castaing and C. Laroche, *J. Physique Lett.* 41(1980) L-283.
55. A. W. Adamson, *A Textbook of Physical Chemistry* (Academic Press, New York, 1973)p. 308.
56. A. W. Adamson, *Physical Chemistry of Surfaces*, 4th ed., (John Wiley, New York, 1982)p. 28.
57. E. Pitts, *J. Fluid Mech.* 63(1974)487.

58. P. Pieranski, *J. Physique* 47(1986)129.
59. P. Pieranski, P. E. Cladis, T. Garel and R. Barbet-Massin,  
*J. Physique* 47(1986)139.
60. R. Kubo, *Statistical Mechanics* (north Holland, Amsterdam, 1967).



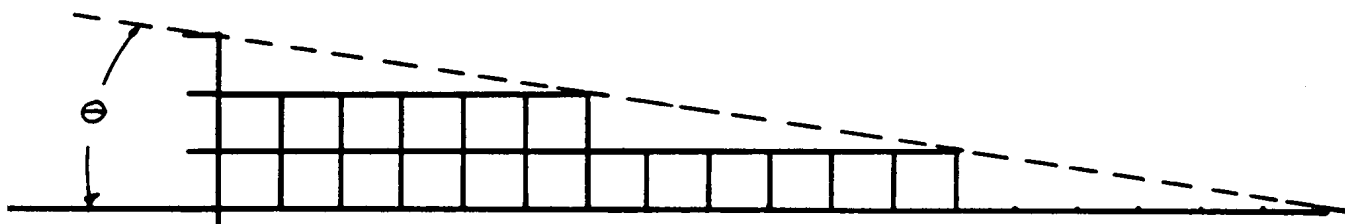


Fig. 1. A two-dimensional simple cubic crystal lattice. The broken line represents a crystal surface with indices (16) and an angle of inclination to the base (horizontal) face (01)  $\theta$ , where  $\theta = \tan^{-1}(1/6)$ .

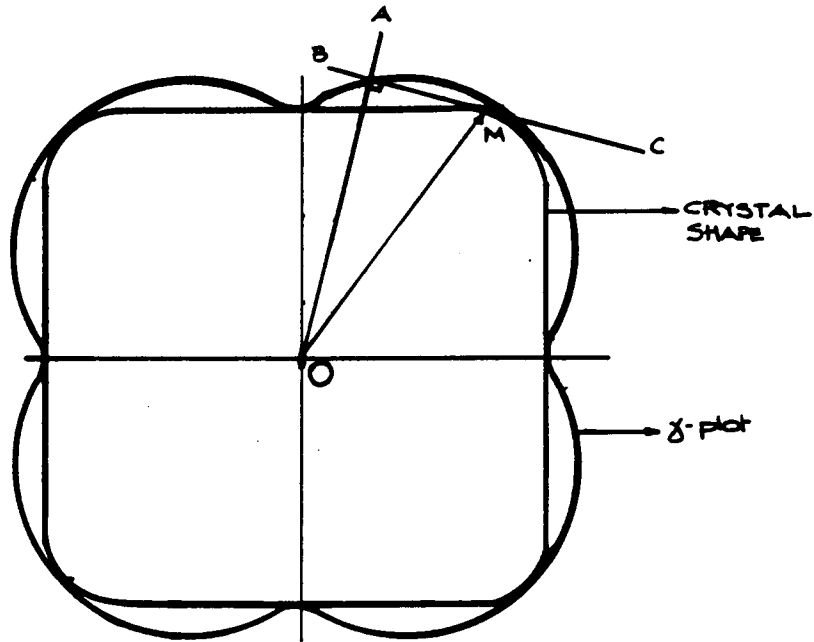


Fig. 2. The Wulff construction in two dimensions. Through point A on the  $\gamma$ -plot with a radius vector  $OA = \gamma(n)n$  from the origin O draw a line (plane) BC normal to  $n$ . The inner envelope of planes like BC, normal to the radii of the  $\gamma$ -plot  $\Gamma$ , gives the equilibrium crystal shape. Note that point M on the crystal surface has surface energy corresponding to point A on the  $\gamma$ -plot.

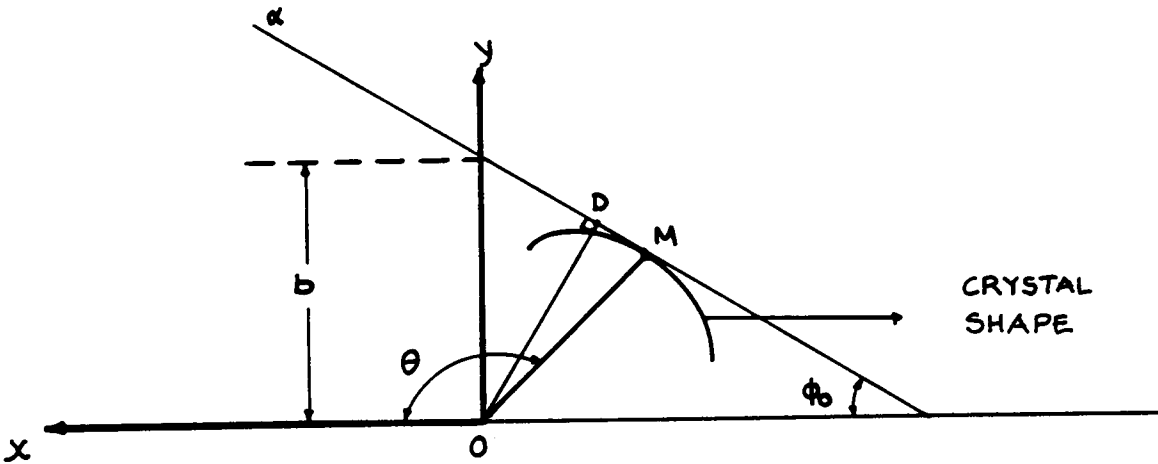


Fig. 3. Geometrical illustration of the derivation of the Wulff construction in two dimensions. A straight line  $\alpha$  with a fixed slope  $p_0$  that belongs to the family (2.21) is drawn. It makes an angle  $\phi_0 = \tan^{-1}(p_0)$  with the positive x-axis and has an intercept  $b = h(p_0)/\lambda$  with the y-axis.  $OD$  is the distance from the origin  $O$  to the straight line and it is equal to  $[h(p_0)/\lambda]\cos(\phi_0) = \gamma(p_0)/\lambda$ . This shows that the distance from the origin to any straight line of the family (2.21), which has as its envelope the ECS, is proportional to  $\gamma(p)$  and that is the Wulff construction.  $OM$  is the distance from the origin to the point  $M$  of the crystal surface given by  $OM = OD/\sin(\theta - \phi_0)$ .

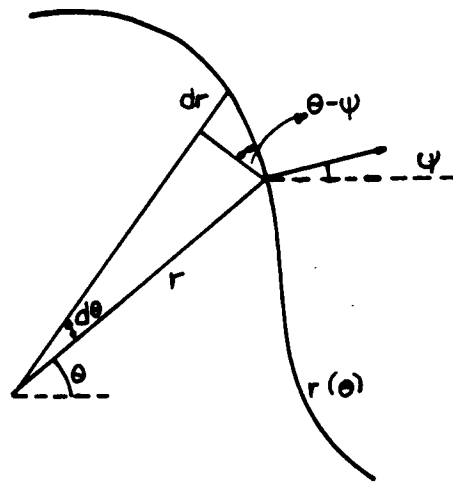


Fig. 4. Geometric construction for the analytic solution. The ECS is given in polar coordinates  $(r, \theta)$ .  $\psi$  is the angle the normal  $n$  makes with the positive x-axis. From the figure follows the dependence of the angle  $\psi$  on  $r(\theta)$ , given by  $\tan(\theta - \psi) = dr/r d\theta$  (after [46]).

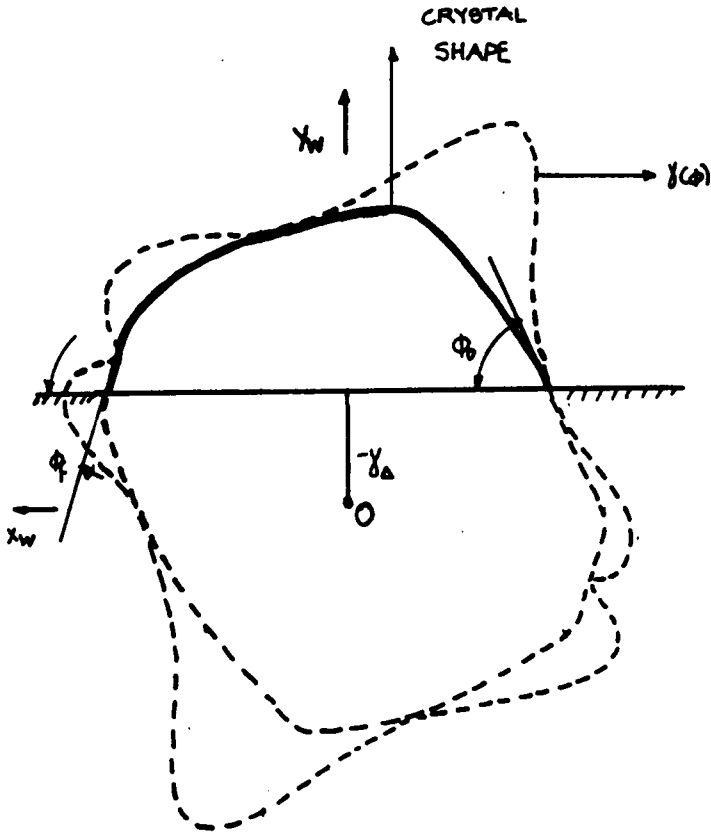


Fig. 5. Wulff-Winterbottom construction for  $\gamma_\Delta < 0$  in two dimensions for an ECS given by  $y = y(x)$ , with the contact angles  $\phi_0$  and  $\phi_f$  identified. For a faceted crystal the contact angles can not be related to a unique value of  $\gamma_\Delta$ .

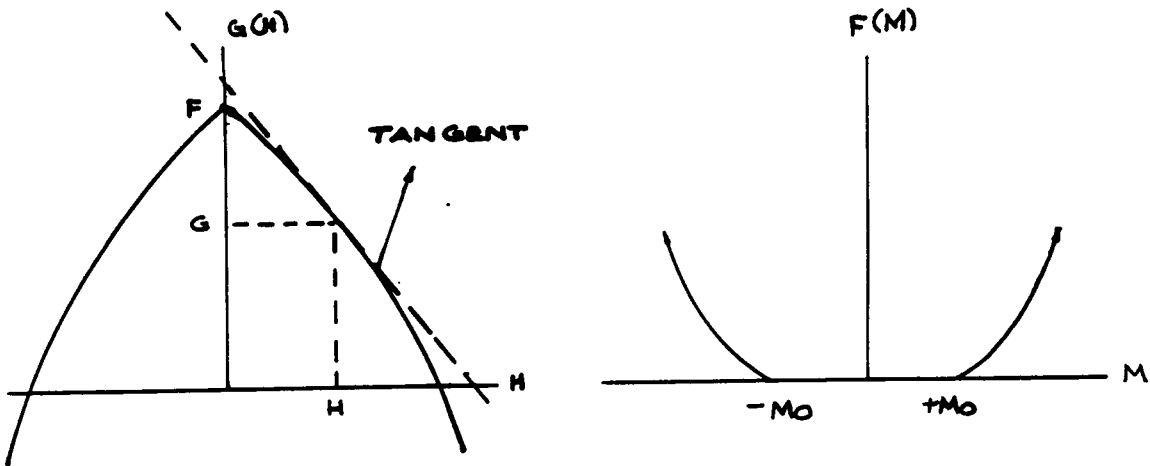


Fig. 6. Geometrical relation between  $G(T,H)$  and  $F(T,M)$  for a ferromagnet at a fixed temperature  $T < T_c$  (after [45,50]).  $H$  is the magnetic field,  $M$  is the magnetization obtained from  $G(T,H)$  by  $M = -(\partial G/\partial H)_T$  and  $T_c$  is the Curie temperature. The tangent to the curve  $G(H)$  at point  $(H, G(H))$  intercepts the  $H = 0$  axis at a height  $F$ , so that  $(F - G)/H = -(\partial G/\partial H)_T = M$  and we obtain the Legendre transformation between  $F(T,M)$  and  $G(T,H)$ . The point to note is that the cusp of  $G(H)$  at  $H = 0$  leads to a region of magnetizations between  $[-M_0, M_0]$  for which  $F(M)$  is not defined. The drawing of the figure utilizes the fact that  $G(T,H)$  is a concave function of the magnetic field  $H$  and  $F(T,M)$  is a convex and even function of the magnetization  $M$  [50].

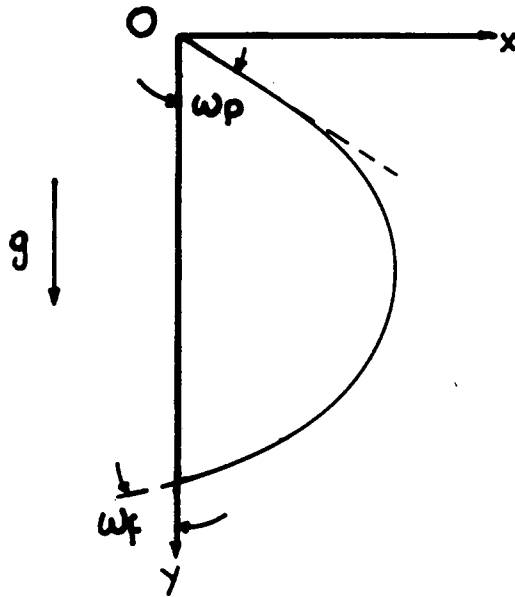


Fig. 7. Crystal pinned at top to a wall in the presence of a gravitational field. The point the crystal is pinned to the wall is taken as the origin of the coordinate system. The position of the wall (substrate) is given by  $x = 0$ . The angles  $\omega_p$  and  $\omega_f$  are the angles the tangent to the ECS makes at the support (pinning) point and at the free end of the crystal with the positive  $y$ -axis. The gravitational force is directed along the positive  $y$ -axis.

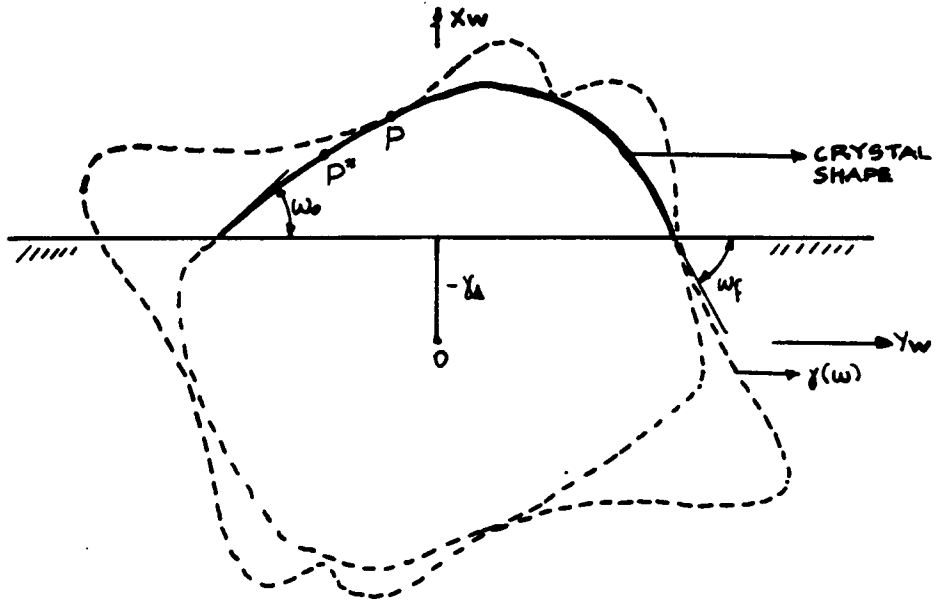


Fig. 8. Wulff-Winterbottom diagram for  $\gamma_\Delta < 0$  in two dimensions for an equilibrium crystal shape  $\Delta$  given by  $x = x(y)$ , with the contact angles  $\omega_b$ ,  $\omega_f$  identified. The points  $P$  and  $P^*$  on the Wulff shape have tangents which make angles  $\omega_b$  and  $\omega_f$  with the positive  $y$ -axis.



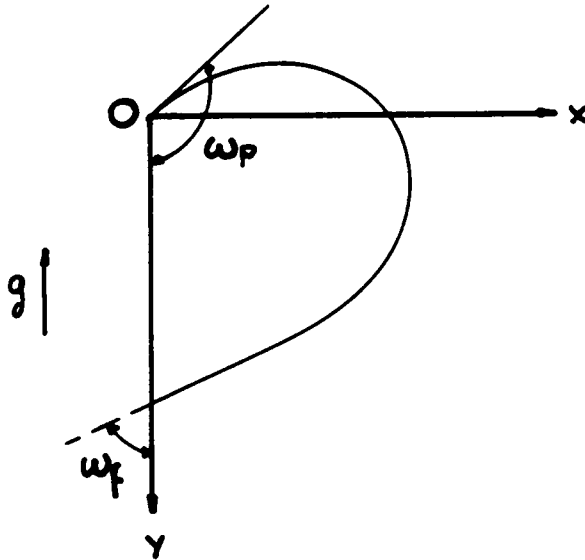


Fig. 9. Crystal pinned at bottom to a wall in the presence of a gravitational field. The case is mathematically identical to that depicted in Fig. 7., but with the direction of the gravitational field reversed. The point of pinning is chosen as the origin  $O$  of the coordinate system and  $\omega_p$  and  $\omega_f$  are the contact angles at the point of support and at the free end of the crystal. The end of the crystal  $y(\phi_f)$  is positive ( $y(\phi_f) > 0$ ).

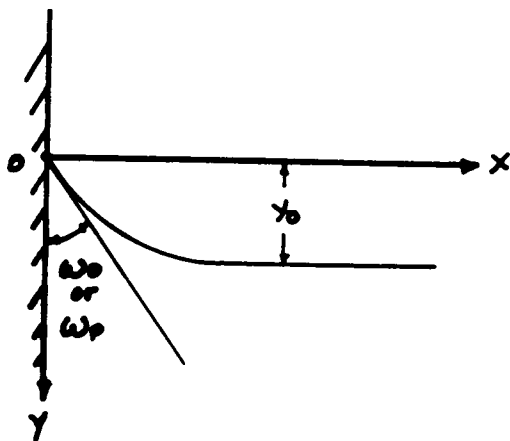


Fig. 10. Meniscus of a semi-infinite crystal or fluid bounded by a vertical plane wall at  $x = 0$  for  $\gamma_{\Delta} < 0$ .  $\omega_0$  is the contact angle of the meniscus with the vertical wall and  $y_0$  is the rise of the wetting meniscus at the wall. Note that the contact point of the meniscus with the wall is taken as the origin of the coordinate system.

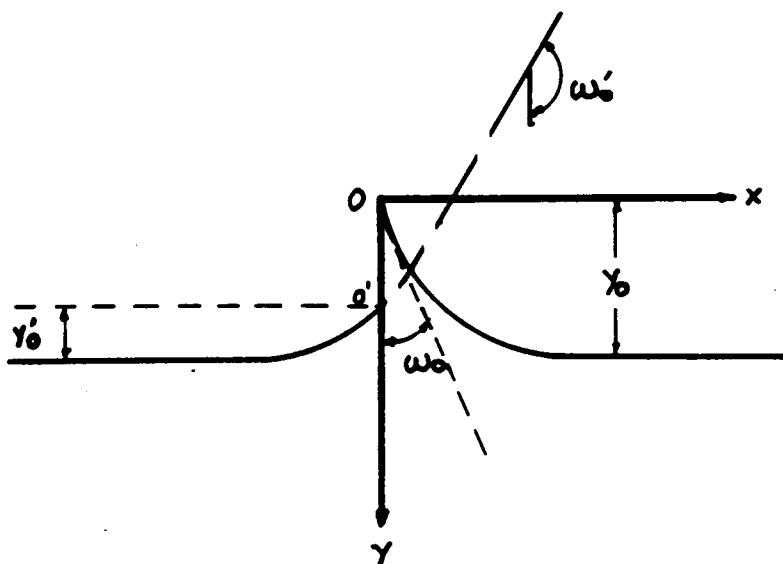


Fig. 11. Wetting ( $\gamma_{\Delta} < 0$ ) semi-infinite crystal menisci separated by a vertical plane wall with both sides the same placed at  $x = 0$ .  $\omega_0$  ( $\omega'_0$ ) is the contact angle with the vertical wall and  $y_0$  ( $y'_0$ ) is the rise at the wall of the meniscus that extends into the  $x > 0$  ( $x < 0$ ) region.

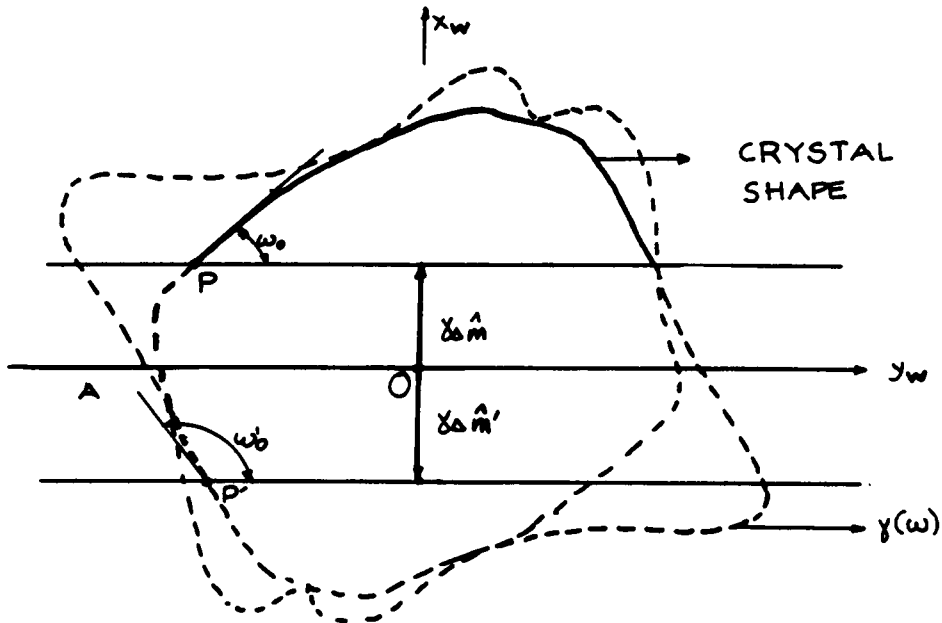


Fig. 12. Wulff-Winterbottom diagram illustrating the determination of the contact angles  $\omega_0$  and  $\omega'_0$  of the two semi-infinite menisci, separated by a vertical wall.  $m$  is the fixed orientation of the wall with respect to the semi-infinite interface that extends into the  $x > 0$  region ( $m = -x$ , where  $x$  is the unit vector in the positive  $x$ -direction) and  $m'$  is the fixed orientation of the wall with respect to the meniscus that lies in the  $x < 0$  region. The points  $P$  and  $P'$  on the Wulff-Winterbottom shape have tangents, which make angles  $\omega_0$  and  $\omega'_0$  with the positive  $y$ -axis. The new orientations, both menisci exhibit when compared to the gravity-free ECS on the same substrate, correspond to the angles the tangents at all points of the portion  $PAP'$  of the Wulff-Winterbottom shape make with the positive  $y$ -axis.

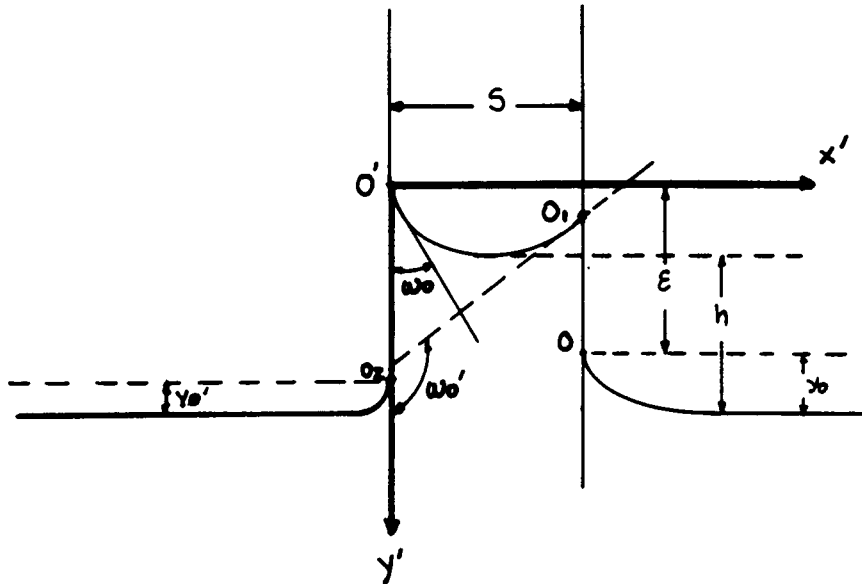


Fig. 13. Two-dimensional wetting meniscus of a crystal between two parallel vertical plane walls.  $\omega$  and  $\omega'$  are the contact angles of the meniscus with the left and right wall with respect to the positive  $y'$ -axis,  $h$  is the meniscus rise between the walls,  $y_0$  is the rise of the semi-infinite meniscus at the right wall and  $\epsilon$  is the difference of the  $y$ -coordinates of the points  $O$  and  $O'$ , where  $O$  is the point of contact of the semi-infinite meniscus with the right wall and  $O'$  is the origin of the coordinate system. Note also that in general, the points of contact  $O'$  and  $O_1$  of the meniscus between the walls with the left and right wall respectively do not have the same  $y$ -coordinate. The same is also true for the points of contact  $O$  and  $O_2$  of the semi-infinite menisci with the right and left wall respectively. This difference between the  $y$ -coordinates of the two pairs of contact points is due to the asymmetry of the  $\gamma$ -plot, as explained in the text. The separation between the walls is  $s$ .

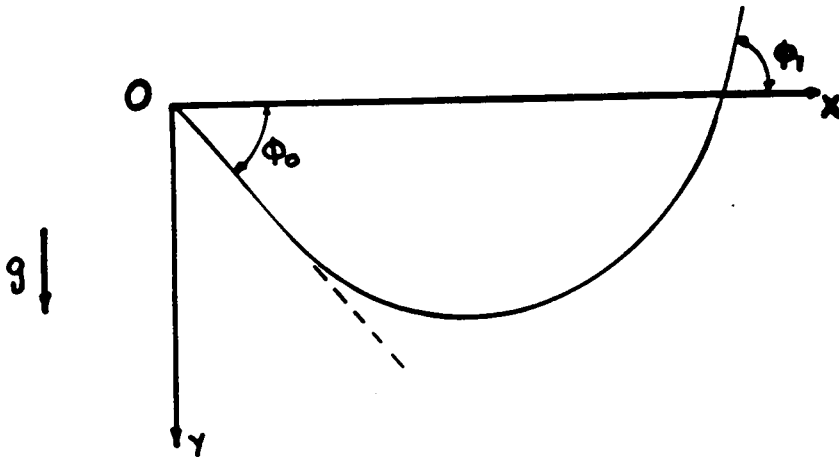


Fig. 14. Crystal hanging from a horizontal support in the presence of a gravitational field (the pendant crystal).  $\phi_0$  and  $\phi_1$  are the contact angles of the pendant crystal at the origin and at the right end respectively, with the positive  $x$ -axis. Gravity is directed along the positive  $y$ -axis.

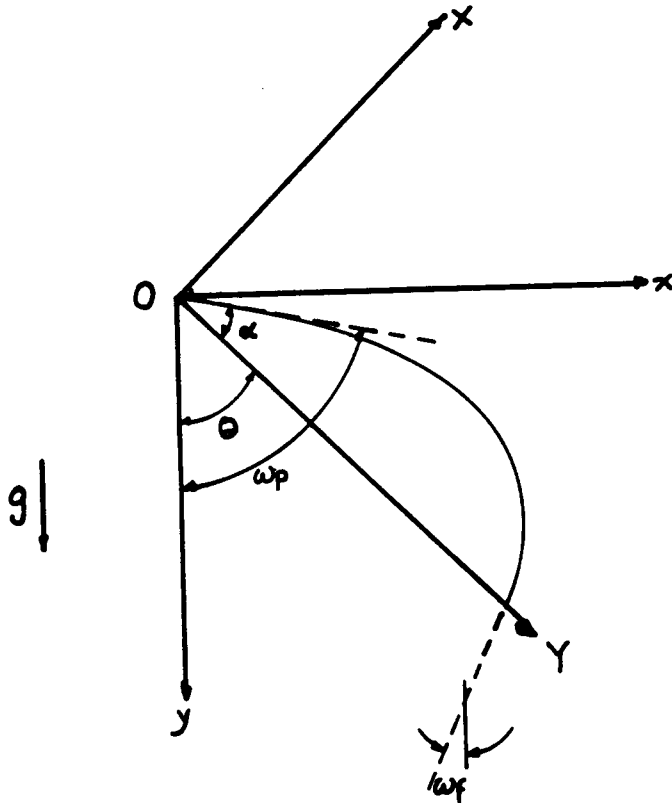


Fig. 15. Crystal supported on an inclined plane in the presence of a gravitational field.  $\omega_p$  and  $\omega_f$  are the angles the tangent to the equilibrium crystal shape makes with the positive  $y$ -axis at the point of pinning and at the free end respectively.  $\alpha$  is the angle the tangent to the ECS makes with the positive  $Y$ -axis and  $\theta$  is the angle between the positive directions of the  $y$ -axis and the  $Y$ -axis. The gravitational field is along the positive  $y$ -axis.

**The two page vita has been  
removed from the scanned  
document. Page 1 of 2**

**The two page vita has been  
removed from the scanned  
document. Page 2 of 2**